PCCP

ROYAL SOCIETY OF CHEMISTRY

REVIEW

View Article Online
View Journal | View Issue

Cite this: *Phys. Chem. Chem. Phys.*, 2024, **26**, 28776

The structural and functional impacts of rationally designed cyclic peptides on self-assembly-mediated functionality

Taichi Kurita [a] and Keiji Numata *[abc]

Compared with their linear counterparts, cyclic peptides, characterized by their unique topologies, offer superior stability and enhanced functionality. In this review article, the rational design of cyclic peptide primary structures and their significant influence on self-assembly processes and functional capabilities are comprehensively reviewed. We emphasize how strategically modifying amino acid sequences and ring sizes critically dictate the formation and properties of peptide nanotubes (PNTs) and complex assemblies, such as rotaxanes. Adjusting the number of amino acid residues and side chains allows researchers to tailor the diameter, surface properties, and functions of PNTs precisely. In addition, we discuss the complex host–guest chemistry of cyclic peptides and their ability to form rotaxanes, highlighting their potential in the development of mechanically interlocked structures with novel functionalities. Moreover, the critical role of computational methods for accurately predicting the solution structures of cyclic peptides is also highlighted, as it enables the design of novel peptides with tailored properties for a range of applications. These insights set the stage for groundbreaking advances in nanotechnology, drug delivery, and materials science, driven by the strategic design of cyclic peptide primary structures.

Received 12th July 2024,
Accepted 10th October 2024

DOI: 10.1039/d4cp02759k

rsc.li/pccp

[a] *Department of Material Chemistry, Graduate School of Engineering, Kyoto University, Katsura, Nishikyo-ku, Kyoto 615-8510, Japan. E-mail: keiji.numata@riken.jp*
[b] *Biomacromolecules Research Team, RIKEN Center for Sustainable Resource Science, 2-1 Hirosawa, Wako, Saitama 351-0198, Japan*
[c] *Institute for Advanced Biosciences, Keio University, Nipponkoku 403-1, Daihouji, Tsuruoka, Yamagata 997-0017, Japan*

1. Introduction

Peptides have revolutionized the biomedical and materials science fields, offering critical benefits such as biodegradability, biocompatibility, and minimal environmental toxicity.[1–5]

Taichi Kurita

Taichi Kurita received his BSc in 2020 (from Prof. Shunsaku Kimura's group) and MSc in 2022 from Kyoto University. Since 2022, he has been a PhD candidate under the supervision of Prof. Keiji Numata in the Department of Material Chemistry, Kyoto University. He is currently a research fellow of the Japan Society for the Promotion of Science (Research Fellowship for Young Scientists). His research interest is the development of polypeptide-based tough materials using rationally designed cyclic peptides.

Keiji Numata

Keiji Numata is currently a Full Professor at the Department of Material Chemistry, Kyoto University; Team Leader at the Biomacromolecules Research Team, RIKEN Center for Sustainable Resource Science; and Project Professor at the Institute for Advanced Biosciences, Keio University, Japan. He is also the Research Director for JST-ERATO Numata Organellar Reaction Cluster Project, Research Director for JST-COI-NEXT, and Research Director for the MEXT Program: Data Creation and Utilization-Type Material Research and Development Project. He investigates the biosynthesis and material design of structural proteins and polypeptides.

Among these, cyclic peptides stand out, drawing significant attention for their unique cyclic topology, which imparts stability superior to that of their linear counterparts.[6–8] Such enhanced stability is critical in pharmaceutical contexts for improving membrane permeability and, consequently, the efficacy of drug delivery systems.[9–13] In the field of materials chemistry, this distinctive cyclic topology facilitates self-assembly into complex structures with advanced functionalities that are unachievable by linear or monocyclic peptides,[14,15] and these self-assembly processes dramatically increase the inherent advantages offered by cyclic peptide topology.

In this review article, we highlight in-depth how strategic modifications in the design of cyclic peptide primary structures determine their assembly behavior and functional outcomes in material chemistry. We investigate peptide nanotube (PNT) formation through hydrogen bonding and complex structures arising from host–guest chemistry, revealing their potential for novel applications. We illustrate these concepts with practical examples, demonstrating the ingenuity underlying the rational design of cyclic peptides. Furthermore, we discuss breakthroughs in structural prediction tools that significantly expand our ability to customize cyclic peptides for precise assembly and applications. Such tools are instrumental in offering predictions that could revolutionize the design of cyclic peptides for breakthrough applications.

A thorough understanding of these principles sets the stage for the development of new cyclic peptide-based materials, increasing their potential for use in sophisticated and targeted functionalities for a variety of applications.

2. Tubular assembly of cyclic peptides

In nature, tubular structures, often composed of proteins, are essential for a variety of biological functions.[16] For example, viruses, such as tobacco mosaic virus, use tubular-shaped structures to infect their hosts and store genetic material.[17] Inspired by these biological activities, engineered nanotubes have potential application prospects in nanomaterials, such as antibiotics, drug delivery, and organic electronics. Recently, several groups have reported the synthesis of molecular nanotubes by forming covalent or noncovalent bonds with biologically relevant compounds. The Harada group developed tubular polymers by crosslinking α-cyclodextrins threaded through polyethylene glycol (PEG) chains (Fig. 1a).[18] Shimizu *et al.* designed glycolipid-like molecules that self-assembled into lipid nanotubes with inner diameters, lengths, and wall thicknesses that could be precisely controlled (Fig. 1b).[19,20] Another example involves the self-assembly of Phe–Phe dipeptides, which is the core sequence of amyloid proteins. These dipeptides form nanotubes or micron-sized tubes with 10 Å hydrophilic channels upon dilution or heating (Fig. 1c).[21] In addition, the amphiphilic block polypeptides have been shown to form nanotubes with a adjustable diameter of approximately 80 nm in Tris-HCl buffer after heat treatment (Fig. 1d).[22]

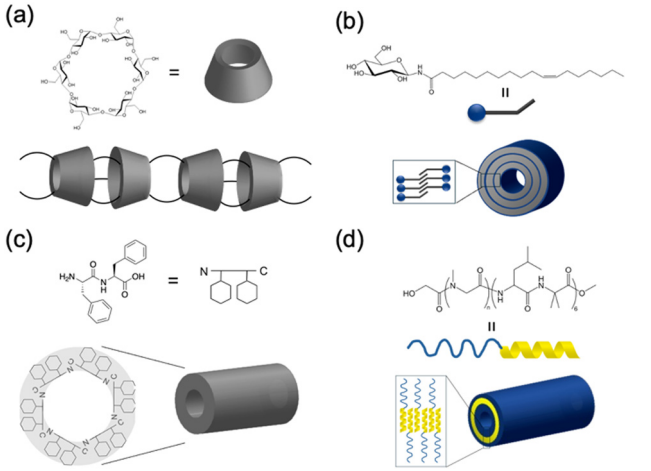

Fig. 1 Schematic illustration of various biomolecular nanotubes: (a) cyclodextrin nanotubes, (b) lipid nanotubes, (c) hydrophilic PNTs, and (d) amphiphilic PNTs.

Among the various methods for constructing tubular assemblies, self-assembling PNTs, which are stacked cyclic peptides stabilized by hydrogen-bonding interactions, are of particular interest because their structural and functional properties can be easily tuned.[14,15,23] Self-assembling PNTs offer two advantages. First, the nanotube diameter can be easily controlled by changing the number of amino acid residues in each cyclic peptide. Second, by varying the amino acid side chains, the outer surface properties of the nanotubes can be easily modified. Thus, nanotubes tailored to specific applications can be prepared by properly designing the constituent cyclic peptides and optimizing the self-assembly conditions. The drawback of constructing PNTs from cyclic peptides lies in the limitations of cyclic peptide synthesis. Two main strategies have been developed for the synthesis of cyclic peptides: cyclization on resin and cyclization in solution. Cyclization on resin is efficient but requires specific side chain groups and several orthogonal protecting groups, whereas cyclization in solution offers more availability in peptide sequences but is more time-consuming due to slower cyclization carried out in dilute solutions and complicated purification steps. Nonetheless, the development of various peptide-ligation technologies over the years has provided valuable tools to overcome these limitations, enabling effective head-to-tail cyclic peptide synthesis.[24] To date, several types of cyclic peptides have been stacked on PNTs and further classified primarily on the basis of their composition as cyclic peptides, including cyclic α-alt(D,L)-peptides (Fig. 2a),[25] cyclic β-peptides (Fig. 2b),[26] and cyclic α,γ-peptides (Fig. 2c).[27] Although these peptides differ in their primary structure, they all have their peptide backbone carbonyl and amide protons oriented perpendicular to the plane of the ring. The formation of PNTs is driven by the ability of adjacent peptide subunits to form β-sheet-like hydrogen bonds across both sides of the ring structure, which is crucial for stabilizing their tubular structures.

2.1. Tubular assemblies of cyclic α-alt(D,L)-peptides

In 1993, Ghadiri *et al.* prepared the first well-characterized PNT using an octapeptide, cyclo[(L-Gln-D-Ala-L-Glu-D-Ala)$_2$].[25]

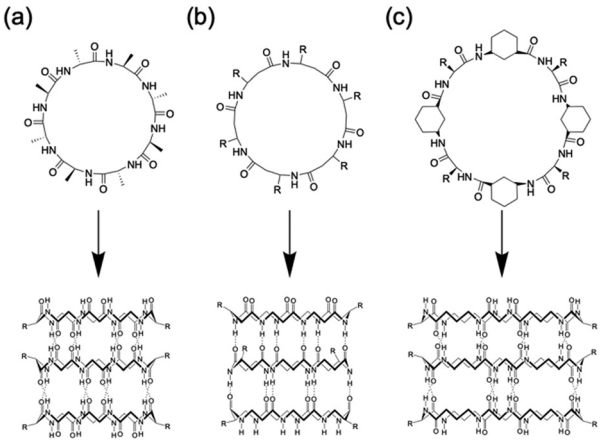

Fig. 2 Classes of cyclic peptides that assemble into PNTs by forming hydrogen bonds: (a) cyclic α-alt(D,L)-peptides, (b) cyclic β-peptides, and (c) cyclic α,γ-peptides.

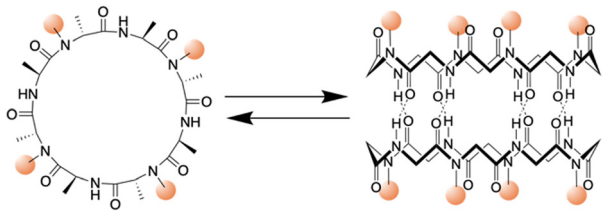

Fig. 3 Schematic illustration of the chemical structure of a cyclic peptide with *N*-methylated amino acids and the cylindrical dimeric ensemble.

This peptide sequence was chosen to increase solubility in basic aqueous solutions and prevent premature subunit association *via* coulombic repulsion. By controlling the acidification of the alkaline peptide solution, rod-shaped microcrystalline aggregates were formed. These structures were subsequently comprehensively characterized *via* transmission electron microscopy (TEM), electron diffraction, Fourier transform infrared (FT-IR) spectroscopy, and molecular modeling.[25] The resulting peptide assemblies featured ordered hollow tubular structures with internal diameters of 7.5 Å and 4.73 Å between the ring-shaped subunits. The cyclic peptide units were stacked in an antiparallel orientation facilitated by backbone–backbone intermolecular hydrogen bonds. Building upon this foundation, Lambert *et al.* employed a similar pH-controlled self-assembly strategy to construct nanotubular microcrystals of a cyclo(D-Phe-L-Asp-D-Phe-L-Asn-D-Phe-L-Asp-D-Phe-L-Asn) that included two aspartic acid units, further advancing the field of PNT design.[28]

Given the versatility of solid- and liquid-phase synthesis methods for producing cyclic peptides with arbitrary sequences, examining the effect of peptide sequence variations on PNTs formation is essential. In natural proteins, minor modifications to the amino acid sequence can drastically alter the biological functions of the resulting protein. Similarly, unique amino acid side chains are anticipated to modulate noncovalent interactions among cyclic peptides, including hydrogen bonding, electrostatic, van der Waals, and hydrophobic interactions. This variety of interactions between various D- and L-amino acid residues could potentially lead to the creation of PNTs with diverse structures and functionalities determined by the primary structures of the corresponding cyclic peptides.

2.1.1. The effect of cyclic peptide primary structures on their stacking behaviors. To gain insight into peptide stacking interactions, selective backbone *N*-alkylation of amino acids with the same chirality was used to facilitate the formation of dimeric motifs (Fig. 3). This approach prevents unlimited stacking by ensuring that all the *N*-methyl groups face the same side of the cyclic peptide. In 1994, Lorenzi *et al.* conducted X-ray crystallography and nuclear magnetic resonance (NMR) studies of the *N*-methylated hexapeptide, cyclo(D-Leu-L-^{Me}*N*-Leu)$_3$, and demonstrated its dimeric antiparallel β-sheet structure in the solid state and deuterochloroform ($CDCl_3$) with a K_a of 80 M^{-1}.[29,30] Similarly, Ghadiri *et al.* reported that the octapeptide cyclo(L-Phe-D-^{Me}*N*-Ala)$_4$ also dimerized under both conditions with a much higher K_a of 2540 M^{-1}.[31] However, the cyclic D,L-α-deca- and cyclic D,L-α-dodecapeptides did not dimerize because of their inability to adopt the required flat conformation. This phenomenon was further explored by Ghadiri *et al.*, who systematically investigated the self-assembly capabilities of 20 cyclic peptides that varied in ring size, backbone alkylation, and amino acid composition.[32] Their findings indicated that only the octapeptide could self-associate in $CDCl_3$, whereas the hexapeptide, as well as the larger decapeptide and dodecapeptide, failed to self-associate owing to the tendency to form hydrogen bonds and increased conformational flexibility, respectively. Further studies on side chain–side chain interactions revealed that cyclic peptides containing homophenylalanine could induce crystal growth through dimer formation. However, a ^{Me}*N*-Phe-containing cyclic peptide did not dimerize due to steric clashes between the backbone *N*-methyl groups and Phe side chains. Similarly, α,α-disubstituted peptides did not form dimers in $CDCl_3$. K_a values were decreased when Phe was replaced with other amino acids, such as Leu, homoallylglycine (Hag), Ile, and Val, which was attributed to increased steric hindrance that affected the binding affinity.

Kobayashi and colleagues examined β-sheet structure formation during the self-assembly of cyclic peptides into PNTs (Fig. 4).[33] Cyclic α-alt(D,L)-peptides can stack into two different β-sheet configurations: parallel and antiparallel. They directly evaluated the thermodynamic preference for antiparallel *versus* parallel β-sheet formation using two enantiomeric forms of the same peptide sequence, cyclo(L-Phe-D-^{Me}*N*-Ala)$_4$ and cyclo(D-Phe-L-^{Me}*N*-Ala)$_4$. In their study, a racemic mixture with an equal amount of each peptide yielded an equilibrium mixture of parallel and antiparallel ensembles distinguishable by ^{1}H NMR spectroscopy. Moreover, the free energy of stabilization was determined for both β-sheet arrangements, and it was revealed that the antiparallel β-sheet structure was thermodynamically more stable than the parallel arrangement by 0.8 kcal mol^{-1}.

Building upon these molecular insights, Silk *et al.* studied the crystallization and structures of two specifically designed cyclic peptides, cyclo(L-Asp-D-Leu-L-Lys-D-Leu)$_2$ and cyclo(L-Asp-D-Ala-L-Lys-D-Ala)$_2$, to understand how side chain variations affect

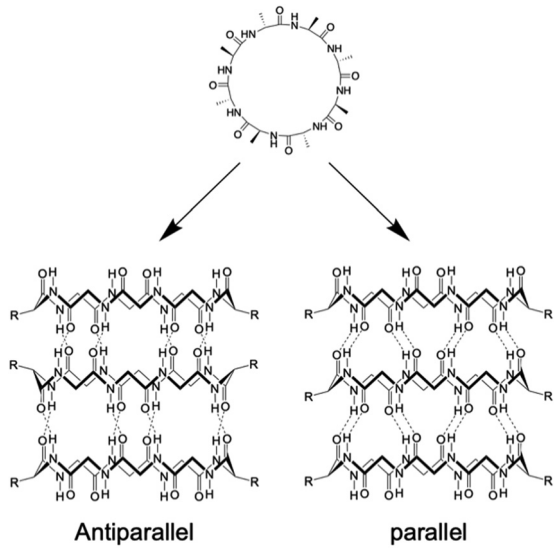

Fig. 4 Schematic illustration of the formation of antiparallel and parallel β-sheet structures from cyclic α-alt(D,L) peptides.

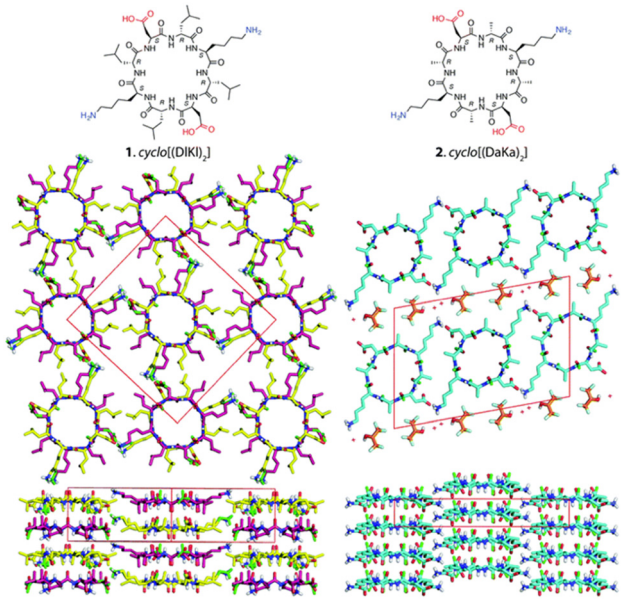

Fig. 5 Chemical structures of cyclo(L-Asp-D-Leu-L-Lys-D-Leu)$_2$ and cyclo(L-Asp-D-Ala-L-Lys-D-Ala)$_2$ and crystal structures of their PNTs. Reproduced with permission from ref. 34 Copyright 2017, The Royal Society of Chemistry.

the stacking arrangements of PNTs (Fig. 5).[34] For cyclo(L-Asp-D-Leu-L-Lys-D-Leu)$_2$, which features larger Leu side chains, the experimental results confirmed the hypothesis that larger side chains facilitate antiparallel stacking. The crystal structure of this cyclic peptide with bulky side chains revealed the formation of continuous β-sheet-like nanotubes with extensive hydrogen bonding interactions between two neighboring peptides. In these structures, the cyclic peptides were aligned in an antiparallel fashion, supporting the idea that larger side chains enhance intermolecular interactions, which ultimately leads to the cyclic peptide adopting a more stable antiparallel orientation. Conversely, crystallographic analysis revealed that cyclo(L-Asp-D-Ala-L-Lys-D-Ala)$_2$, which contains shorter side chains like Ala, adopted a parallel stacking arrangement. The shorter side chains facilitated closer packing of the nanotubes, which was hypothesized to be conducive for parallel β-sheet formation. These findings underscore the critical roles of side chain size and composition in determining the stacking manner of the cyclic peptides. The contrasting stacking behaviors observed for these two peptides, driven by differences in side-chain characteristics, illustrate a fundamental aspect of peptide design for engineering materials with specific structural and functional properties.

2.1.2. The effect of cyclic peptide primary structures on the orientation of PNTs. To assess the influence of hydrophobic interactions on the orientation of nanotubes in the solid state, Ghadiri *et al.* designed cyclic peptide subunits incorporating nonpolar amino acids such as Ala, Val, Leu, and Phe (Fig. 6).[35] They investigated hydrophobic interactions specifically by synthesizing and examining four cyclic peptides: cyclo(L-Gln-D-Ala)$_4$, cyclo(L-Gln-D-Val)$_4$, cyclo(L-Gln-D-Leu)$_4$, and cyclo(L-Gln-D-Phe)$_4$. This comprehensive approach involving multiple amino acid variants allowed an exploration of the effectiveness of side chain hydrophobic and hydrogen bonding interactions in nanotube crystal engineering. These four cyclic peptides formed needle-shaped microcrystals under controlled conditions and were analyzed by low-dose cryogenic electron microscopy, FT-IR spectroscopy, electron diffraction, and molecular modeling. All the samples displayed highly ordered axial periodicities ranging from 4.75 to 4.85 Å, which is consistent with an ideal antiparallel β-sheet arrangement. However, the lateral assembly of PNTs varied among cyclic peptides. Cyclo(L-Gln-D-Leu)$_4$ and cyclo(L-Gln-D-Phe)$_4$ exhibited tighter packing than cyclo(L-Gln-D-Ala)$_4$ did, whereas cyclo(L-Gln-D-Val)$_4$ exhibited

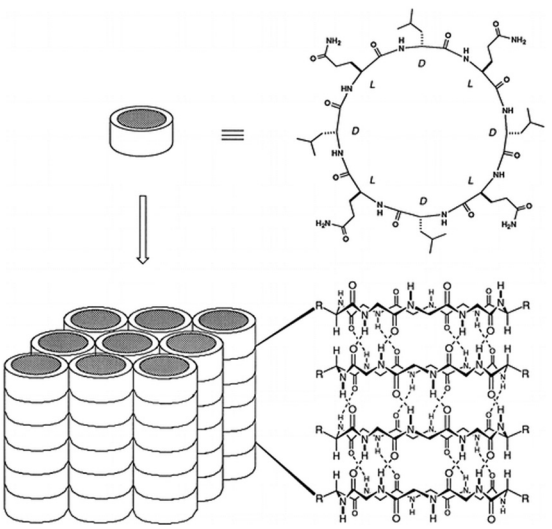

Fig. 6 Schematic illustration of the formation of ordered parallel arrays of solid-state nanotubes from cyclic peptide structures with alternating D- and L-amino acids. The arrangement is dependent on the peptide sequence and conditions used. Reproduced with permission from ref. 35 Copyright 1996, American Chemical Society.

less ordered lateral packing. Such variation indicates that the peptide sequence significantly influences the lateral packing of the nanotubes rather than the vertical stacking of the cyclic peptide subunits. These findings underscore the pivotal role of hydrophobic and hydrogen-bonding interactions in directing the assembly of PNTs and suggest that more ordered self-assembling structures can be produced through the rational design of cyclic peptide sequences.

Recent advances in supramolecular chemistry have demonstrated that rational design of the primary structure of cyclic peptides can lead to the generation of highly ordered and functional self-assembled structures. In particular, the works of the Montenegro group exemplify how strategic molecular design can facilitate the formation of complex supramolecular architectures from simple peptide units.[36,37] In 2019, Insua *et al.* explored cyclic peptides that feature specific amino acid sequences with alternating D and L chirality, cyclo(D-Leu-L-Trp-D-Leu-L-His-D-Glu-L-Gln-D-His-L-Glu) (Fig. 7a).[36] This design is crucial for guiding peptides to first assemble into one-dimensional nanotubes and subsequently into two-dimensional nanosheets. These peptides were composed of tailored hydrophobic and hydrophilic domains. The hydrophobic domain, which typically contained amino acids such as Leu and Trp, formed the internal hydrophobic core of nanotubes, which is essential for their structural stability. The hydrophilic domain, comprising charged and polar amino acids, such as Glu and His, facilitates external interactions, enabling the nanotubes to remain soluble and interact to form larger structures. These cyclic peptides adopt a β-sheet secondary structure that aids in the formation of cylindrical nanotubes, which are crucial for subsequent lateral packing into stable 2D nanosheets. Expanding on this foundation, Insua and Montenegro recently designed cyclo(L-Trp-D-Leu-L-Glu-D-His-L-Leu-D-Trp-L-Leu-D-Glu-L-His-D-Leu) (Fig. 7b).[37] The introduced Trp residues acted as hydrophobic supramolecular hinges, enhancing control over their self-assembly process. These hinges allow the peptides to fold and organize more effectively and reach a critical polymerization threshold where lateral stacking becomes favorable, thus forming robust 2D networks. The precise placement of hydrophobic and hydrophilic residues, along with the structural flexibility provided by Trp hinges, allows for the controlled, dynamic assembly of peptides into monolayers that can adapt to environmental changes. Together, these studies underscore the importance of amino acid sequence and chirality when designing cyclic peptides that self-assemble into higher-order structures. By manipulating these parameters, researchers can create peptides that self-assemble into predetermined geometries and exhibit certain functional properties, such as responsiveness to external stimuli. This innovative approach holds great promise for the development of new materials with applications in biosensing, molecular transport, and responsive surfaces, reflecting a profound understanding of how molecular design can influence the macroscopic material properties.

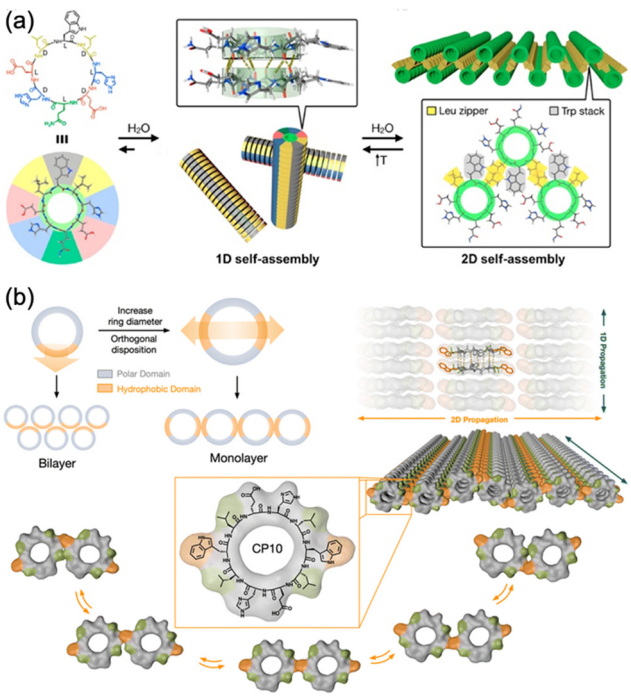

Fig. 7 (a) Proposed model for the sequential 1D-to-2D self-assembly of cyclo(D-Leu-L-Trp-D-Leu-L-His-D-Glu-L-Gln-D-His-L-Glu). Reproduced with permission from ref. 36 Copyright 2020, American Chemical Society. (b) Rational design and structural scheme of self-assembling 2D nanotubular monolayers of cyclo(L-Trp-D-Leu-L-Glu-D-His-L-Leu-D-Trp-L-Leu-D-Glu--L-His-D-Leu). Reproduced with permission from ref. 37 Copyright 2023, The Royal Society of Chemistry.

2.1.3. Summary. Cyclic peptides composed of an even number of alternating D- and L-amino acids can adopt a flat conformation, with the amide N–H and C=O bonds oriented perpendicular to the ring. As a result, they form PNTs *via* stacking of cyclic peptides through hydrogen bonds. As long as they consist of an even number of alternating D- and L-amino acid residues, a wide range of peptide sequences is compatible. As shown in Table 1, the stacking mode and lateral aggregation of PNTs varied depending on these amino acid sequences. While assemblies of 1D fibers and 2D sheets have been reported so far, the rational design of cyclic peptides is expected to provide access to a wide variety of other well-ordered self-assembled structures.

2.2. Tubular assemblies of cyclic β-peptides

As significant structural counterparts to cyclic α-alt(D,L)-peptides, cyclic β-peptides, which are derived from β-amino acids, show a pronounced ability to form stable PNTs. β-Peptides are notable for their structural integrity, strong resistance to enzymatic degradation and advantageous conformational properties, which may provide benefits compared with α-peptides.[38] In 1997, Seebach *et al.* were the first to synthesize and characterize cyclic β-peptides.[39] They designed and synthesized three stereoisomeric cyclic β-tetrapeptides composed of 3-amino butanoic acids, specifically cyclo(β^3-HAla)$_4$. Studies on cyclo(β^3-HAla)$_4$ confirmed that these peptide structures maintain a flat conformation with each subunit interconnected through four hydrogen bonds. Moreover, the rings stack efficiently due to the spatial configuration and hydrogen bonding capabilities of β-amino acids, resulting in tightly bound nanotubes. This precise molecular arrangement

Table 1 A summary of cyclic α-alt(D,L)-peptide sequences, along with the structures and functions of the resulting PNTs

Section	Peptide sequence	Characteristic feature	Key sequences	Ref.
2.1.	Cyclo(L-Gln-D-Ala-L-Glu-D-Ala)$_2$	First example of PNT formation	Alternating sequences of D- and L-amino acids	25
	Cyclo(D-Phe-L-Asp-D-Phe-L-Asn-D-Phe-L-Asp-D-Phe-L-Asn)	Acidification triggered PNT formation	Asp (pH-response)	28
2.1.1.	Cyclo(D-Leu-L-^{Me}*N*-Leu)$_3$	Dimmer formation (K_a = 80 M^{-1} in $CDCl_3$)	*N*-Methylation of Leu	29 and 30
	Cyclo(L-Phe-D-^{Me}*N*-Ala)$_4$	Dimmer formation (K_a = 2540 M^{-1} in $CDCl_3$)	Number of amino acid residues in the cyclic peptide (8-mer had higher K_a than 6-mer)	31
	Cyclo(L-Phe-D-^{Me}*N*-Ala)$_4$ Cyclo(D-Phe-L-^{Me}*N*-Ala)$_4$	Measuring the relative stability of parallel *vs.* antiparallel β-sheets	Replace chirality of the constituent amino acids	33
	Cyclo(L-Asp-D-Leu-L-Lys-D-Leu)$_2$	Antiparallel stacking arrangements	Side chain interactions between adjacent nanotubes	34
	Cyclo(L-Asp-D-Ala-L-Lys-D-Ala)$_2$	Parallel stacking arrangements		
2.1.2.	Cyclo(L-Gln-D-Ala)$_4$		Hydrophobicity of cyclic peptides (The intertubular hydrophobic interactions affected orienting nanotubes.)	35
	Cyclo(L-Gln-D-Val)$_4$	Less ordered lateral packing		
	Cyclo(L-Gln-D-Leu)$_4$	Tighter lateral packing of nanotubes than cyclo(L-Gln-D-Ala)$_4$		
	Cyclo(L-Gln-D-Phe)$_4$	Tighter lateral packing of nanotubes than cyclo(L-Gln-D-Ala)$_4$		
	Cyclo(D-Leu-L-Trp-D-Leu-L-His-D-Glu-L-Gln-D-His-L-Glu)	2D nanosheets	Amphiphilic sequence Leu zippers and Trp stacks	36
	Cyclo(L-Trp-D-Leu-L-Glu-D-His-L-Leu-D-Trp-L-Leu-D-Glu-L-His-D-Leu)	2D nanotubular monolayers	Amphiphilic sequence The positioning of two opposite hydrophobic 'tryptophan hinges'	37

led to the formation of a structure with an inner pore of approximately 2.6 Å in diameter.

The most distinctive feature of PNTs composed of β-amino acids is their ability to generate a significant macrodipole moment along their longitudinal axes. This is a result of the uniform orientation of all the amide bonds in the cyclic skeleton facing the same direction. Macrodipoles have been shown to accelerate electron transfer reactions along their orientation.[40–42] Driven by the hypothesis that macrodipoles resulting from the stacking of cyclic β-peptides might enhance their performance as artificial transmembrane ion channels, Ghadiri *et al.* investigated the ion transport capabilities of cyclic β-peptides.[43] They used three homochiral cyclic β-tetrapeptides, cyclo(β^3-HTrp)$_4$, cyclo(β^3-HTrp-β-HLeu)$_2$, and cyclo(β^3-HLeu)$_4$, to explore functionalities beyond the C_2 symmetrical conformation reported by Seebach, which features a collapsed central hole in the peptide ring. Instead, they suggested that these cyclic β-tetrapeptides assume a C_4 symmetrical conformation that maintains an internal diameter of 2.6–2.7 Å within a lipid membrane environment. Notably, cyclo(β^3-HTrp)$_4$ achieved an ion transport rate of 1.9×10^7 K$^+$ ions per second, which is on par with that of the previously studied cyclic α-alt(D,L)-peptide cyclo[(L-Trp-D-Leu)$_3$-L-Gln-D-Leu]. This performance is particularly important, given the much smaller internal diameter of the nanotube compared with its cyclic α-alt(D,L)-peptide counterpart, which typically measures 7–8 Å. This finding highlights the potential role of the macrodipole in influencing ion transport efficiency. However, a direct comparison between cyclic β-peptides and cyclic α-alt(D,L)-peptides with similar chemical structures and internal diameters is essential to draw a definitive conclusion.

In addition to their advantages in ion transport, the significant macroscopic dipole moments of PNTs indicate their potential applications in organic electronic nanomaterials with pyroelectric, piezoelectric, and semiconducting properties. However, two substantial challenges must be addressed to effectively utilize PNTs as valuable nanomaterials. The first challenge involved modifying the PNT surface to align the functional groups in a consistent pattern. The second challenge is achieving precise structural control when constructing the PNT bundles, as cyclic β-peptide PNTs tend to form bundles with a wide size distribution; this phenomenon is driven by strong dipole–dipole interactions due to the significant dipole moments along their axes. Here, we highlight the strategic approach applied by the Kimura group in the design of cyclic peptides to overcome these challenges.

2.2.1. The effect of cyclic peptide primary structures on side chain alignment on PNT surfaces. PNTs have been functionalized by incorporating charge carriers, such as several aromatic groups.[44–46] Despite this advancement, the alignment of these functional groups along the PNT remains predominantly random, which is attributed to the presence of rotational isomers among the stacked cyclic peptides. Thus, a regular side-chain arrangement could significantly increase the potential of PNTs as scaffolds for one-dimensional functional molecular arrays. Various studies have described methods for regulating side-chain orientation by modulating their interactions. One such method controls the stacking direction *via* electrostatic (salt bridge) interactions. For example, when stacking D,L-alternating cyclic octa-α-peptides with Lys and Glu residues, salt bridges form between the Lys and Glu residues of the adjacent peptides in the PNT, which leads to the regular alignment of the pyrene[47] and fullerene[48] side chains along the PNT. However, these methods require the incorporation of certain functional groups into the primary sequence of the cyclic peptides. Therefore, the development of a new approach that does not depend on the introduction of specific groups is

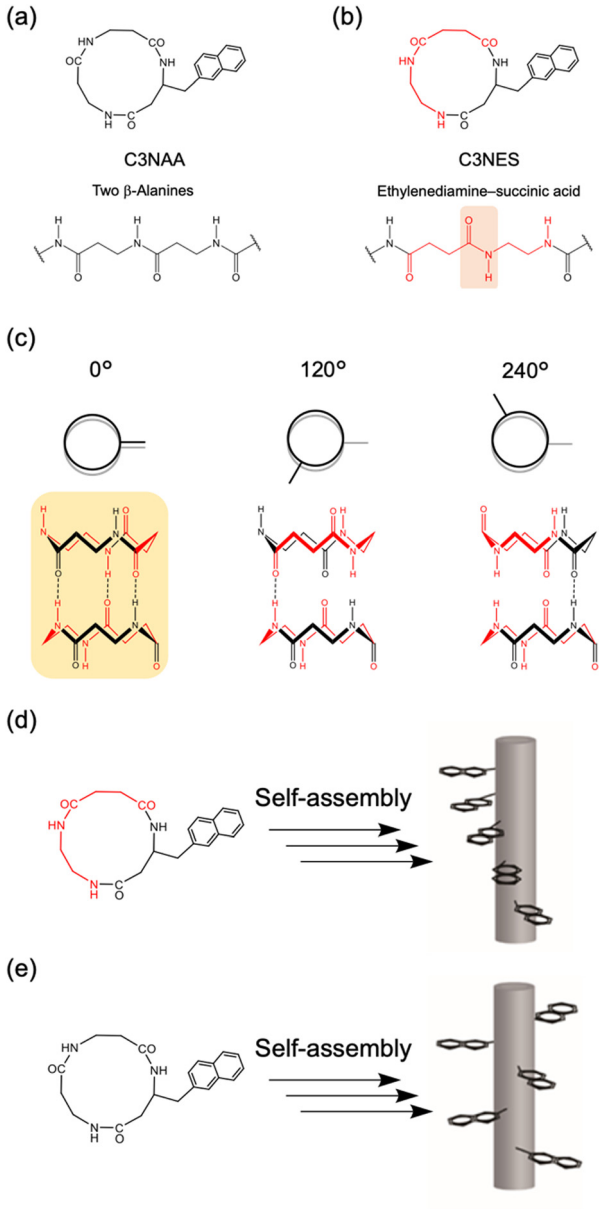

Fig. 8 Molecular structures of cyclic tri-β-peptides of (a) C3NAA and (b) C3NES. (c) Structures of C3NES dimers, which have a sequence with initial rotations of 0°, 120°, and 240°. Schematic of PNTs formed from cyclic β-peptides with (d) or without (e) a sequence of ethylenediamine-succinic acid.

essential for the regular alignment of side chains along the PNT surface.

To achieve oriented stacking of cyclic peptides, Tabata *et al.* designed a new cyclic peptide containing a sequence of ethylenediamine (ED) and succinic acid (SA), cyclo(β-Ala(nap)-ED-SA) (C3NES) (Fig. 8a and b).[49,50] This sequence differs from that of its analog, cyclo(β-Ala(nap)-β-Ala-β-Ala) (C3NAA), in the orientation of the connecting amide bond. The former sequence enabled the formation of optimal intermolecular hydrogen bonding interactions along the PNT, but only when the cyclic peptides were stacked such that the ED-SA units were aligned

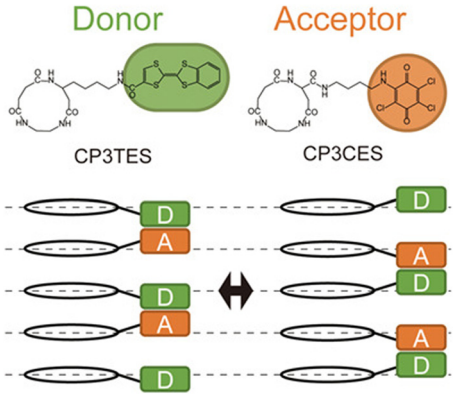

Fig. 9 Chemical structures of cyclic peptides and schematic of the switch pairing of the charge–transfer complexes along the PNT accompanying the change in direction of the dipoles. Reproduced with permission from ref. 51 Copyright 2020, Wiley-VCH.

on the same side of the nanotube (Fig. 8c). Such alignment results in the side chains being located on the same side of the PNT (Fig. 8d and e). Ohmura *et al.* designed cyclic peptides incorporating sequences of ED and SA, which were functionalized with the donor tetrathiafulvalene (TTF) and acceptor molecules (chloranil), specifically cyclo(β-Lys(TTF)-ED-SA) and cyclo(β-Asp(chloranil)-ED-SA), from which PNTs were constructed (Fig. 9).[51] This design facilitated the linear alignment of TTF and chloranil along the nanotube axis and led to the generation of molecular dipole switching materials. This approach allows dipole switching without structural modifications, thereby ensuring minimal energy dissipation.

Cyclic β-peptide-based PNTs exhibit a piezoelectric response due to the tilting of the amide bonds under an applied electric field (Fig. 10). In the emerging era of the internet of things (IoT), where sensors are essential for health monitoring, piezoelectric materials such as PNTs are prized for their ability to convert mechanical motion into electrical energy, which is ideal for miniaturized sensors and power sources.[52,53] Recent advancements have focused on downsizing organic piezoelectric nanogenerators to sizes smaller than 1 μm.[54–56] These devices minimally affect human activities and adapt well to the curved and corrugated surfaces of human organs. Leveraging their self-assembling and biocompatible properties, cyclic β-peptide-based PNTs have shown great potential in the development of piezoelectric devices ranging in size from several to tens of micrometers.

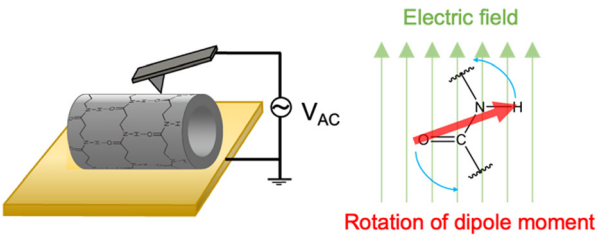

Fig. 10 Schematic illustration of the mechanism of the piezoelectric properties of PNTs on a gold substrate.

To assess the effect of side chain orientation on the piezoelectric properties of PNTs, two types of PNTs were evaluated: those composed of C3NAA with randomly oriented side chains and those composed of C3NES with aligned side chains.[57] The C3NAA nanotube bundles demonstrated a high converse piezoelectric coefficient, d_{33}^*, of approximately 9 pm V^{-1}. In contrast, the C3NES nanotube bundles exhibited a limited response to the applied electric field, with a d_{33}^* value of less than 1 pm V^{-1}. This variation in the piezoelectric coefficient can be attributed to the extent of the non-centrosymmetric arrangement of peptide dipoles. In the case of the C3NAA nanotubes, all peptide bonds were unidirectionally aligned, leading to a highly non-centrosymmetric dipole distribution within the PNT. Conversely, in the C3NES nanotubes, two consecutive hydrogen bonding networks adopted an antiparallel orientation, disrupting the noncentrosymmetry and reducing the piezoelectric coefficient. These findings align with observations from other cyclic β-peptide-based nanotubes, where reduced symmetry typically enhances the piezoelectric properties.[58]

2.2.2. The effect of cyclic peptide primary structures on PNT bundle structure. PNTs composed of cyclic β-peptides in which all amide bonds point in the same direction along the nanotube to generate a large dipole along the nanotube have a strong tendency to associate and form thick PNT bundles because the dipole–dipole interactions between PNTs causes them to adopt an antiparallel orientation. Therefore, it is challenging to prepare a single PNT or a bundle of PNTs with a defined number. Ishihara *et al.* designed amphiphilic cyclic tri-β-peptides composed of *trans*-2-aminocyclohexylcarboxylic (ACHC) acid and β-glucosamino acid (GA), cyclo[$(GA)_2$ACHC], to control the association number of PNTs in a bundle (Fig. 11a).[59]

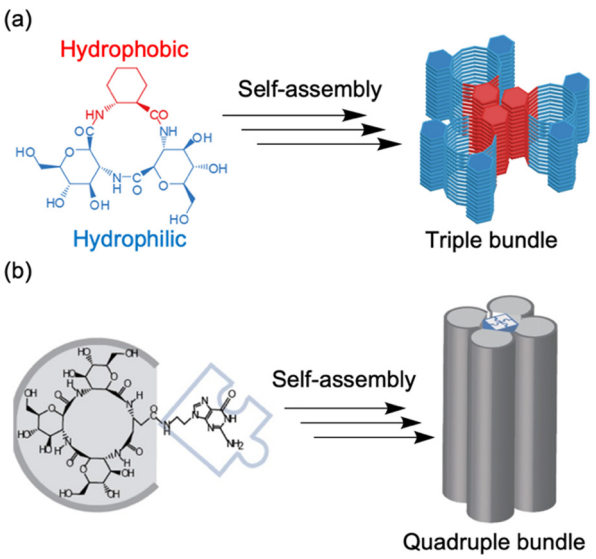

Fig. 11 (a) Schematic illustration of the association of three amphiphilic cyclic tri-β-peptides. The hydrophobic cyclohexyl side chains were aligned linearly to make the surface hydrophobic. The other surface is hydrophilic, which leads to PNT association. (b) Schematic of self-assembly processes, from a cyclic tetra-β-peptide with a guanine moiety to a quadruple PNT bundle. Reproduced with permission from ref. 60 Copyright 2013, Wiley-VCH.

The amphiphilic molecular structure of the peptide contributed to the association of the three molecules into a trimeric unit. Ishihara *et al.* also designed a tetra-β-cyclic peptide composed of three GA units and a β-Glu with a guanine (G) moiety attached to its side chain, cyclo[$(GA)_3$-β-Glu(G)]. This nucleobase forms a hydrogen-bonded G-quartet in the presence of metal, mainly potassium, ions. They used this property to induce the cyclic peptide to self-assemble in water upon the addition of potassium chloride to generate bundles of four nanotubes due to the formation of G-quadruplexes (Fig. 11b).[60] However, the construction of single PNTs is difficult.

Recently, the introduction of charged side-chain moieties to cyclic β-peptides was found to lead to the formation of single PNTs in aqueous solutions, preventing bundle formation by electrostatic repulsion.[61] To prevent ionic functional groups from affecting the piezoelectric properties of PNTs, the authors focused on a helical peptide, which has a dipole moment from the C-terminus to the N-terminus, generating an electrostatic potential field.[62] The authors designed CP3A8E, a cyclic β-peptide with a helical peptide attached to its side chain, to lead the formation of a single PNT (Fig. 12).[63] A single PNT was constructed from CP3A8E by preventing close contact between the PNTs owing to the electrostatic repulsion and steric hindrance provided by the helical peptides. This study highlights the role of the primary structure of a cyclic peptide in controlling the hierarchical structure of the resulting PNT. Additionally, after this single PNT was constructed, we were able to compare its piezoelectric properties with those of PNT bundles. Piezoresponse force microscopy (PFM) measurements revealed that the d_{33}^* of the single PNTs was 1.39 ± 0.12 pm V^{-1}. This value closely matches the d_{33}^* value of 1.34 ± 0.16 pm V^{-1} measured for bundled PNTs.[58] These results indicate that the piezoelectric properties of PNTs are inherently linked to the deformation of their cyclic skeletons rather than their aggregate structure. In other words, the piezoelectric properties of PNTs remain unchanged when their size is reduced to a single unit. Given that a single PNT with a size of 4 nm represents the smallest known biomaterial-based piezoelectric material, PNTs composed of cyclic peptides are promising candidates for use

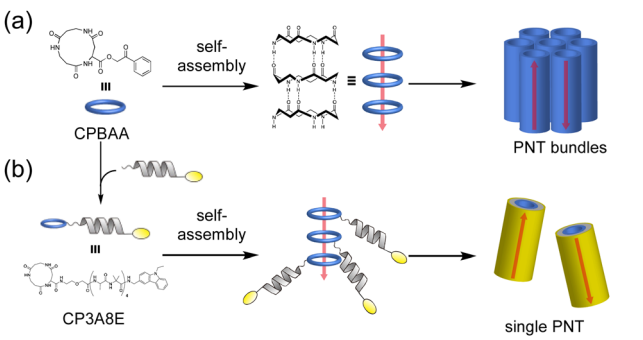

Fig. 12 (a) Schematic illustration of PNT bundle formation with a usual cyclic β-peptide. (b) Schematic of single PNT formation from a cyclic β-peptide with a helical peptide. Each red arrow indicates the dipole moment of the PNT. Reproduced with permission from ref. 63 Copyright 2021, American Chemical Society.

as energy harvesters in biomedical applications, particularly in previously inaccessible microenvironments.

2.2.3. Cyclic β-peptide containing sugar units. Fujimura *et al.* developed a novel class of cyclic β-peptides with pyranose rings derived from sugar-based amino acids as side chains, which displayed significantly increased solubility due to the presence of multiple hydroxyl groups (Fig. 13a).[64,65] These water-soluble cyclic β-peptides form nanotubes with specific affinity sites for proteins, especially lectins.[66] Increasing the number of amino acid residues in the cyclic peptides caused the inner pore diameter of the nanotubes to increase. For example, a PNT composed of cyclic hexamers of GA had an inner pore diameter of approximately 5.1 Å, which is sufficient to accommodate guest molecules such as PEG, leading to the formation of a pseudorotaxane (Fig. 13b).[65] This complex is particularly effective in aqueous environments, where hydrophobic interactions expedite the threading process, unlike the slower formation observed in mixed water and ethanol solutions. Threading occurs through each ring sequentially, facilitated by the water medium to promote rapid nanotube assembly through intermolecular hydrogen bonding with PEG. A unique feature of this system is the stability of the pseudorotaxane without stoppers at the axle terminals, which is attributed to the multiple interaction sites and hydrophobic interactions between the hydrogen bond-stabilized nanotube and PEG.

2.2.4. Summary. The most distinctive feature of PNTs composed of β-amino acids is their ability to generate macrodipole moments along their longitudinal axes. This property significantly enhances their ion transport capabilities and opens up potential applications in various nanomaterials, such as piezoelectric and electronic devices. Recent advances in cyclic peptide design have facilitated the assembly of PNTs with precise control over side chain alignment and bundle size. This development has led to more sophisticated and functional nanostructures, suitable for diverse applications, as outlined in Table 2. Furthermore, the introduction of sugar units in cyclic peptides has led to the development of a new class of PNTs that are effective in aqueous environments, expanding their potential utility in biological applications.

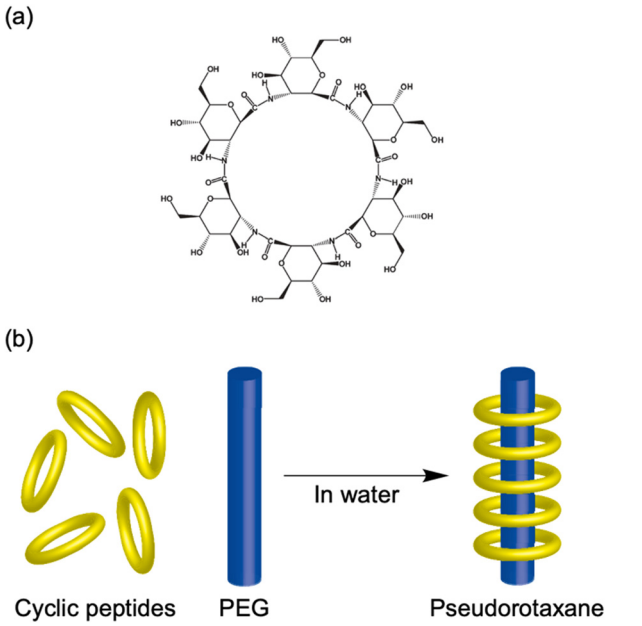

Fig. 13 (a) Chemical structures of cyclic hexamers of β-glucosamino acid. (b) Schematic illustration of polypseudorotaxane formation from cyclic hexamers of β-glucosamino acid and poly(ethylene glycol).

2.3. Tubular assemblies of cyclic α,γ-peptides

Recent advancements in peptide-based materials have led to significant interest in the development of PNTs featuring alternating α- and γ-amino acids. Granja *et al.* pioneered the use of cyclic γ-amino acids, such as *cis*-3-aminocycloalkane carboxylic acid (γ-Aca), to create novel self-assembling cyclic peptides.[27] These cyclic γ residues confer unique structural and functional properties to PNTs, enabling their diverse applications in biological systems and materials science. The incorporation of cyclic γ-amino acids contributes to the rigid and flat conformation of the peptide backbone, which is essential for stacking and nanotube formation. This structural orientation also endows the internal cavity with novel features, such as the creation of a hydrophobic region within the otherwise hydrophilic lumen. This effect was achieved by strategically positioning a cycloalkane methylene group from γ-Aca into the lumen of the nanotube. In contrast to α- or β-peptide-based nanotubes, which have fixed cavities, γ-cyclic PNTs permit functional modifications at specific sites within the nanotubes, thus offering enhanced control over their internal properties. PNTs are typically composed of an even number of α- and cyclic γ-amino acids arranged in a planar ring-like conformation, which facilitates selective intermolecular interactions. This configuration promotes antiparallel stacking, driven by specific hydrogen bonding patterns between the amide groups of the α and γ residues, potentially resulting in more stable nanotube structures. Alternatively, parallel arrangements facilitated by interactions between the α-face and γ-face are also possible, which contributes to the stability of these assemblies. The ability to fine-tune the peptide rings and hydrophobicity of the internal cavity through simple chemical modifications enhances the utility of these assemblies, positioning them as versatile candidates for diverse material science and biotechnological applications.

2.3.1. The effect of cyclic peptide primary structures on homo- and hetero dimer formation. Dimeric assemblies have also been prepared from *N*-methylated cyclic α–γ-peptides, in which hydrogen bond donation from one face of the ring structure was strategically blocked through *N*-methylation, similar to that in cyclic α-alt(D,L)-peptides. In 2003, Granja *et al.* reported the first examples of *N*-methylated cyclic hexapeptides composed of γ- and D-α-amino acids, cyclo(D-Phe-^{Me}*N*-γ-Aca)$_3$ and cyclo(γ-Aca-D-^{Me}*N*-Ala)$_3$. These cyclic peptides formed dimers based on α–α or γ–γ interactions, respectively. A noteworthy finding related to *N*-methylated cyclic α–γ-peptides was that heterodimers were formed when mixing 3-aminocyclohexanecarboxylic

Table 2 A summary of cyclic β-peptide sequences, along with the structures and functions of the resulting PNTs

Section	Peptide sequence	Characteristic feature	Key sequences	Ref.
2.1.	Cyclo(β^3-HAla)$_4$.	First example of PNT from cyclic β-peptides	β-Pepitde	39
2.1.1.	Cyclo(β^3-HTrp)$_4$	Working as transmembrane ion channels	Cyclic β^3-peptides adopted flat-ring C_4 symmetrical conformation with an internal diameter of 2.6–2.7 Å, large enough to accommodate water and small ions.	43
	Cyclo(β^3-HTrp-β-HLeu)$_2$,	Working as transmembrane ion channels		
	Cyclo(β^3-HLeu)$_4$	Not working as transmembrane ion channels	β^3-HTrp residues allowed PNTs incorporation into lipid membranes.	
2.2.1.	Cyclo(β-Ala(nap)-ED-SA) (C3NES)	The side chains located on the same side of the PNTs.	ED-SA sequences	49 and 50
	Cyclo(β-Ala(nap)-β-Ala-β-Ala) (C3NAA)	The side chains were randomly distributed along the PNTs.		
	Cyclo(β-Lys(TTF)-ED-SA) and cyclo(β-Asp(chloranil)-ED-SA)	Formation of charge–transfer complexes	Linear alignment of donor and acceptor molecules induced by ED-SA sequences	51
2.2.2.	Cyclo[(GA)$_2$ACHC]	Triple bundle formation of the PNTs	Amphiphilic cyclic β-peptide	59
	Cyclo[(GA)$_3$-Glu(G)]	Quadruple bundle formation of the PNTs	Introducing a guanine group into a cyclic peptide	60
	CP3A8E	Formation of single PNTs	Introducing a helical peptide into a cyclic peptide	63
2.2.3	Cyclo(GA)$_6$	Pseudorotaxane formation with PEG	Cyclic hexa-β-peptide of GA with large inner pore of 5.1 Å and water solubility	65

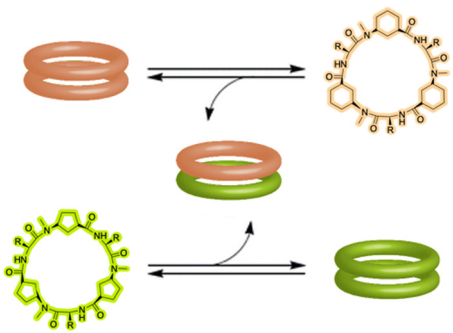

Fig. 14 Heterodimeric supramolecular systems. The α,γ-Ach and α,γ-Acp cyclic peptide combination was used to obtain new heterodimeric structures.

acid (Ach)-based hexapeptides, cyclo(D-Phe-(1*R*,3*S*)-^{Me}*N*-γ-Ach)$_3$, with *cis*-3-aminocyclopentanecarboxylic acid (Acp)-based hexapeptides, cyclo(D-Leu-(1*R*,3*S*)-^{Me}*N*-γ-Acp)$_3$, rather than the corresponding homodimers (Fig. 14).[67] This enhanced stability, with the heterodimers being approximately 30 times more stable than their homodimeric counterparts, underscores the efficiency of the backbone-to-backbone interaction strategy. A critical aspect of this molecular architecture is that heterodimer formation predominantly relies on interactions at the level of the peptide backbone rather than on the side chain interactions typical of biological systems. This focus on backbone interactions allows for selective heterodimer formation and facilitates the modification of side chain properties. By anchoring diverse functional groups to side chains, these cyclic peptides can be customized to perform various functions, including systems that are active in electron or energy transfer.[68]

2.3.2. Internal functionalization of PNTs induced by γ-amino acid. The functionalization of the β-carbon of the cycloalkane moiety in the γ-residue can tailor the internal properties of the resulting tubular assembly. These nanotubes are products of precise molecular engineering that strategically functionalize this specific carbon. Such a design ensures that the functional groups are *trans*-oriented relative to the carboxylic and amino groups of the peptide. Consequently, the side groups project into the cavity of the nanotube in a pseudoequatorial orientation, which is crucial for maintaining the integrity of the self-assembly process. In practice, cyclic α–γ-peptide containing 4-amino-3-hydroxytetrahydrofuran-2-carboxylic acid (γ-Ahf), cyclo(D-Leu-^{Me}*N*-γ-Acp-D-Leu-γ-Ahf-)$_2$, was synthesized.[69,70] This approach enables the formation of dimers and larger peptide assemblies that fold into specific shapes or form spherical aggregates upon interaction with targeted anions such as chloride and nitrate, highlighting their adaptability. The presence of hydroxyl groups within the nanotube cavity influences their internal properties, directing self-assembly and enhancing the stability of the formation. Moreover, such modification allows the nanotube to function as a selective anion transporter, an innovation that diverges from traditional cation-selective PNTs.[69,70] For example, introducing *N*-methylated Ahf residues prevents unwanted folding and instead promotes the assembly of dimeric structures that trap polar molecules, such as methanol or water, which reflects the hydrophilic nature of the modified cavity. Moreover, the flexibility of the PNT was enhanced by additional functionalization, such as the incorporation of picolinic acid moieties through ester linkages, which altered their interaction capabilities.[71] This modification facilitates the recognition and encapsulation of various molecules, including metal ions and organic acids, within the dimer cavity, significantly altering the properties of both the nanotube and guest molecules. Advanced applications, such as attaching Zn–porphyrin to cyclic peptides to form molecular cages that selectively bind and encapsulate large ligands, have demonstrated the ability of these functionalized nanotubes to be adapted for specific molecular interactions.[72] This degree of

Table 3 A summary of cyclic α,γ-peptide sequences, along with the structures and functions of the resulting PNTs

Section	Peptide sequence	Characteristic feature	Key sequences	Ref.
2.3.1.	Cyclo(γ-Aca-D-^{Me}N-Ala)$_3$	First example of PNT from cyclic α,γ-peptides with γ–γ hydrogen bonding interactions	Alternating sequences of α- and γ-amino acids	39
	Cyclo(D-Phe-^{Me}N-γ-Aca)$_3$	First example of PNT from cyclic α,γ-peptides with α–α hydrogen bonding interactions		
	Cyclo(D-Leu-(1*R*,3*S*)-^{Me}N-γ-Acp)$_3$ Cyclo(D-Phe-(1*R*,3*S*)-^{Me}N-γ-Ach)$_3$	Heterodimer formation	Combination of Acp- and Ach-based cyclic α,γ-peptides	67
2.3.2.	Cyclo(D-Leu-^{Me}N-γ-Acp-D-Leu-γ-Ahf)$_2$	PNTs with hydrophilic cavity	γ-Ahf	69 and 70

customization opens new avenues for the use of PNTs in sophisticated drug delivery systems and biosensing technologies and the creation of functional materials tailored for specific biochemical and industrial applications.

2.3.3. Summary. The introduction of γ-amino acids significantly enhances the diversity of cyclic peptides, enabling the construction of PNTs with functions that cannot be achieved with either cyclic α-alt(D,L)-peptides or cyclic β-cyclic peptides, as summarized in Table 3. By selecting the appropriate γ-amino acids, *N*-alkylated cyclic α,γ-peptides formed heterodimers more preferentially than homodimers. Furthermore, functionalizing γ-amino acids allows for the modification of internal properties of the resulting PNTs, such as altering the hydrophobicity of the nanotube cavity. These modifications lead to enhanced properties, including selective anion transport and the encapsulation of various molecules. These developments establish cyclic α,γ-peptide-based PNTs as promising candidates for applications in drug delivery, biosensing, artificial ion channels and the development of functional nanomaterials.

3. Supramolecular chemistry of cyclic peptides

3.1. Cation binding ability of cyclic peptides

The three-dimensional structures of naturally occurring cyclic peptides are closely related to their biological activities.[73–76] Cyclization constrains the molecule overall, preconfiguring it for receptor binding and reducing the conformational entropy loss by this preconfiguration. Additionally, this reduction in entropy loss aids in complex formation. For example, the cyclodecapeptide antibiotic antamanide forms complexes with alkali metal cations, particularly potassium ions.[77] Similarly, the cyclodepsipeptide valinomycin transports alkali metal cations across biological membranes after complex formation.[78–81] These cation interactions have a significant influence on biological activity, promoting the synthesis of various synthetic peptides inspired by their natural counterparts. Researchers have evaluated the complex-forming abilities of these synthetic peptides and determined their conformations. Although researchers have studied the structures and affinities of individual cyclic peptides, not all combinations can be synthesized, leaving design guidelines imperfectly established. Pro plays a crucial role in the activity of these peptides.[82–88] Pro is found in many naturally occurring peptide antibiotics and peptide antitoxins.[89,90] Thus, it is beneficial to consider the structural implications of including Pro in cyclic peptides, because its pyrrolidine ring promotes the formation of a bend in the peptide chain, and this bending can restrict or halt the coordination of adjacent amide nitrogen donors to the metal ions. The rigidity imposed by the N–C_α bond in proline residues limits the formation of β-turns and restricts the available conformations. Therefore, Pro is frequently used in the design of synthetic cyclic peptides.

3.2. Rotaxanes and catenanes from cyclic peptides

Complex formation significantly affects biological functions, a topic that is further detailed in other reviews.[91] We believe that utilizing the receptor properties of cyclic peptides enables the formation of supramolecular assemblies with interlocked structures, such as rotaxanes. This is evident from the crucial role of crown ethers, which can also coordinate cations, in supramolecular chemistry.[92] In nature, peptide [2]rotaxane systems exhibit specific bioactivities. Notably, peptide-based rotaxane microcin J25, one of the few natural molecules that inhibits RNA polymerase, is an ideal target for antimicrobial therapy.[93–95] By synthesizing analogs that mimic these properties, we can potentially obtain new bioactive compounds with considerable utility. Furthermore, lasso peptides possess unique properties that make them suitable for various applications in medicinal chemistry and can serve as robust scaffolds. In addition, rotaxane crosslinked polymers are extremely tough owing to their freely movable crosslinking points, which equalize the tension in the polymer chain upon tensile deformation.[96,97] Rotaxanes synthesized from peptides can serve as crosslinkers, increasing the toughness of the network polymers while exhibiting biodegradability and compatibility with polypeptides and proteins. Therefore, interlocking peptide structures are expected to have various applications. However, the methods by which interlocked structures, such as rotaxanes and catenanes, can be synthesized from cyclic peptides remain limited owing to specific technical and molecular constraints.

Aucagne *et al.* used cyclo(L-Pro-L-Gly)$_{4and5}$, which reported to form a γ-turn structure with its carbonyl oxygens pointing toward the center of the ring, demonstrating high affinity constants for metal ions and cations in acetonitrile.[88] They reported the formation of [2]rotaxanes with yields of 56–63% *via* the construction of cationic diol threads and utilization of bulky acid chlorides to "stopper" the reactions with these macrocycles *via* ethane-1,2-diammonium and butane-1,4-diammonium templates (Fig. 15).[98]

All peptide-based rotaxanes have not been reported because peptides lack binding motifs with sufficient strength for stable

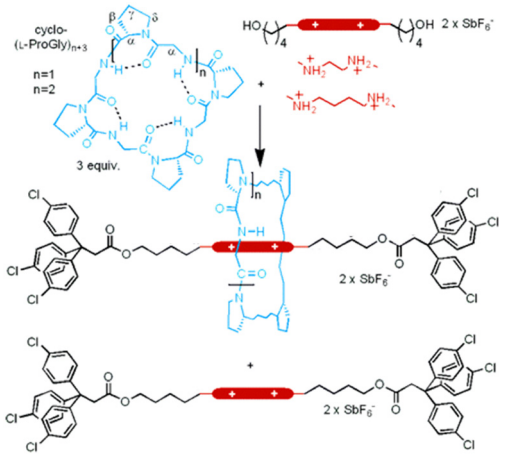

Fig. 15 Synthetic scheme of cyclic peptide-based [2]rotaxanes from cyclo(PG)$_4$ and diammonium threads. Reproduced with permission from ref. 98 Copyright 2006, American Chemical Society.

rotaxane formation.[99] Specific cyclic peptides can form assemblies through hydrogen bonding interactions between amide bonds. However, these bonds are not strong enough to allow axial molecules to penetrate the cyclic peptides.

The authors found that cyclo(L-Pro-L-Gly)$_4$ forms complexes with primary amines *via* hydrogen bonding. Bearing this in mind, we successfully synthesized all peptide-based rotaxanes from cyclic peptides with a γ-turn structure, electrophiles, and nucleophiles *via* the active-template method[100] (Fig. 16).[101] This method facilitates the synthesis of rotaxanes through an axis-forming reaction inside a cyclic molecule. The successful synthesis of the peptide rotaxane was confirmed by high-performance liquid chromatography (HPLC) and electrospray ionization mass spectrometry (ESI-MS) in a yield of 1.2%. Combining experimental results with molecular dynamics (MD) simulation data, we determined that cyclic peptides with an inward-directed carbonyl oxygen and a spacious internal cavity are preferable for rotaxane synthesis.

Recent advances in peptide-based catenane formation have been reported using dynamic combinatorial libraries. These supramolecular systems are generated from reversible binding units that self-assemble around a specific receptor target, acetylcholine. Specifically, chiral dipeptides with a masked aldehyde functionality and hydrazide moiety (*e.g.*, Pro–Phe) reversibly bind *via* hydrazone bonds. Surprisingly, among the potential diastereomers, only [2]catenane, consisting of two interlocked macrocyclic trimers, was formed.[102] The acetylcholine trimethylammonium group was identified as the major template recognition site.

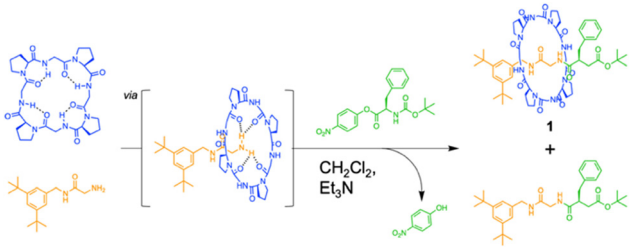

Fig. 16 Synthesis of an all peptide-based [2]rotaxane by the cyclic peptide-accelerated *N*-acylation of primary amines. Reproduced with permission from ref. 101 Copyright 2024, American Chemical Society.

The relatively limited number of peptide-based rotaxanes and catenanes available clearly indicates ample room for further experimental and theoretical investigations in these intriguing fields. Peptide science is classically an interdisciplinary field that is expected to contribute significantly to bridging and strengthening the connection between synthetic organic chemistry, biology, and nanoscience. Within this framework, the unique modular nature of peptides and vast chemical diversity of natural and unnatural amino acids offer substantial advantages for the development and application of peptide-based rotaxanes and catenanes. Mechanically interlocked peptides and proteins exhibit unique properties that are not observed in conventional proteins, including thermal, mechanical, and chemical stability; proteolytic resistance; and dynamic features such as sliding and switching. A synthetic approach to generating interlocking structures opens new avenues for the creation of peptide- and protein-based materials with unprecedented functions.

4. Solution structure prediction of cyclic peptides *via* computational methods

As mentioned above, a wide variety of assemblies have been constructed *via* rational design of cyclic peptide primary structures, and various functions have been achieved. If we can predict the solution structures of cyclic peptides and the types of complexes that they form with various molecules, we can more easily and rationally design novel cyclic peptides on the basis of their predicted solution structures. These cyclic peptides are likely to form novel assemblies and perform innovative functions.

Cyclic peptides tend to adopt multiple conformations in solution, which complicates the generation of structural models. This difficulty arises because experimental measurements, such as NMR and circular dichroism (CD) spectroscopy, often yield time- and ensemble-averaged data. Therefore, computational methods play a crucial role in studying the conformational ensembles of cyclic peptides and could provide insights that are challenging to obtain experimentally.

MD simulations are powerful tools for understanding the properties of peptides and proteins. However, conventional MD simulations often struggle to provide complete structural ensembles of cyclic peptides because of the large free energy barriers between conformations that are caused by ring strain. To overcome these barriers, several enhanced sampling methods have been developed, including replica exchange molecular dynamics (REMD),[103] bias-exchange metadynamics (BE-META),[104] multivariate molecular dynamics (McMD),[105] accelerated molecular dynamics (aMD),[106] and complementary coordinate molecular

dynamics (CoCo-MD).[107] Please refer to this review article for a discussion on the enhanced techniques used for sampling cyclic peptide conformations and the recent applications of MD simulations used with these methods to understand or design cyclic peptides.[108] Owing to the development of these enhanced sampling techniques, it is now possible to study dozens of cyclic peptide sequences that target essential transitional motions within a reasonable timeframe. In addition to explaining known experimental results, MD simulations have recently played a leading role in making predictions, which have been subsequently verified experimentally.[109–111] Lin *et al.* identified that conformational switches in cyclic peptides require coherent changes in coupled dihedral angles-specifically, either the ϕ and ψ angles of the same residue (ϕ_i and ψ_i) or the ψ angle of a residue and the ϕ angle of the next residue (ψ_i and ϕ_{i+1}).[112] By targeting these coupled dihedrals using two-dimensional collective variables with BE-META simulations, they significantly reduced convergence times compared to standard methods, enhancing the efficiency of sampling conformational space. Expanding on this method, they systematically investigated more than 70 cyclic pentapeptides, aiming to understand how amino acid sequences control their structural ensembles, and developed a scoring function based on these MD simulation data to predict structural preferences, estimating that cyclo(L-Gly-L-Asn-L-Ser-L-Arg-L-Val) adopt a well-defined $\beta_{II'} + \alpha_R$ conformation (a type-II′ β-turn with a tight α_R turn opposing it). Further MD simulations confirmed this prediction, revealing 67% prevalence of the desired conformation. This result was further supported by NMR experiments.[109] Extending the application of this predictive BE-META simulation, they explored the comprehensive structural ensembles of two families of cyclic hexapeptides: cyclo(L-Gly$_n$-L-Ala$_{\{6-n\}}$) and cyclo(L-Gly$_n$-L-Val$_{\{6-n\}}$). These two families contain a total of 27 cyclic peptides, taking into account sequence permutations and symmetry. Among these cyclic peptides, cyclo(L-Val-L-Val-L-Gly-L-Gly-L-Val-L-Gly) was uniquely predicted to adopt a single, highly populated conformation characterized by two β_{II} turns at specific residues.[113] They synthesized cyclo(L-Val-L-Val-L-Gly-L-Gly-L-Val-L-Gly) and confirmed the MD predictions using NMR spectroscopy, observing the anticipated well-defined structure. Additional simulations and experiments underscored the critical role of the Val residue at position 1 in stabilizing this conformation, emphasizing the significance of specific amino acid positions for structures of cyclic peptides.[110] MD simulations also play a predictive role in designing new cyclic peptides as potential inhibitors of protein–protein interactions. The optimized BE-META sampling protocol accurately predicted the preorganized structure of a series of peptides, each with individual amino acid substitutions in a Kelch-like ECH-associated protein-1 (Keap1)-binding sequence derived from nuclear factor-erythroid 2 p45-related factor 2 (Nrf2). The experimental binding affinity results confirmed the binding affinity prediction using a simulated conformational ensemble. The culmination of their sequence optimization effort, cyclo(*ortho*-L-Cys-L-Asn-L-Pro-L-Glu-L-Thr-D-Ala-L-Glu-L-Cys), competes with the highest reported binding affinity for Keap1 to date (4.7 nM, compared to 2.8 nM for a disulfide-linked cyclic peptide of similar size[114]), indicating that MD simulations can design substitutions that promoted the desired conformations more effectively.[111]

Recent advancements in machine learning (ML) technologies, particularly the development of AlphaFold2 and RoseTTAFold, have demonstrated impressive capabilities for predicting protein structures.[115–120] A notable extension of this technology is AfCycDesign, which is based on AlphaFold and has shown promising results in predicting the structures of cyclic peptide monomers, underscoring the adaptability of these models to various molecular configurations.[121] However, cyclic peptides, typically comprising 5 to 15 amino acids, rarely form stable secondary structures or distinct folds, which presents significant challenges for these ML models in terms of accurately predicting the peptide structure in solution. Moreover, advanced ML models, which were developed with extensive protein-specific structural and evolutionary data, are not directly applicable to cyclic peptides. Cyclic peptides often lack detailed structural data owing to limited nuclear Overhauser effect (NOE) signal availability and are commonly produced through nonribosomal synthesis. This scarcity in data complicates the further enhancement of these models for such applications. Furthermore, because the training data for these models are derived primarily from proteins, predicting the structures of peptides that incorporate unnatural amino acids or exist in nonaqueous environments remains difficult. The pioneering work of the Lin group on structural ensembles achieved by MD and ML (StrEAMM) marked a significant advancement in the computational prediction of cyclic peptide structures.[122] This innovative method combines MD simulations with ML techniques to predict the structural ensembles of cyclic peptides effectively. By performing MD simulations on 705 variants, they compiled a diverse dataset to train linear regression models. This approach enables the rapid prediction of structural ensembles of cyclic pentapeptides, giving results in less than one second per sequence across an extensive sequence space of approximately 150 000 potential pentapeptides (Fig. 17). To extend this approach, StrEAMM has been adapted for cyclic hexapeptides. They incorporated advanced ML techniques, including convolutional and graph neural networks, to capture nonlinear interactions, and these techniques significantly outperformed traditional models. These enhanced StrEAMM models demonstrated remarkable prediction accuracies, with R^2 values reaching 0.97 for pentapeptides and 0.91 for hexapeptides.[123]

5. Conclusion and future outlook

Our comprehensive review underscores the transformative role of the primary structures of cyclic peptides, highlighting their profound impact on self-assembly processes and functionality (Fig. 18). This insight propels our ability to manipulate these structures, paving the way for the development of sophisticated biomaterials and groundbreaking nanotechnology. Strategically modifying peptide sequences, particularly the ring sizes and side

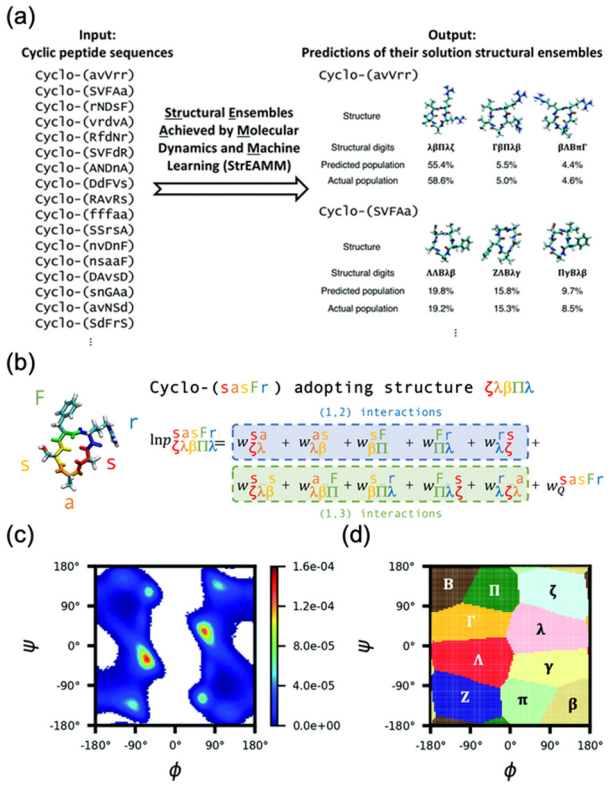

Fig. 17 Schematic illustration of StrEAMM. (a) A StrEAMM model leverages MD simulation results as the training dataset to rapidly predict the structural ensembles of cyclic peptides with both well-structured and non-well-structured sequences. (b) the StrEAMM linear regression models to predict the population for a sequence cyclo($X_1X_2X_3X_4X_5$) adopting a specific structure $S_1S_2S_3S_4S_5$. The natural logarithm of the population of cyclo($X_1X_2X_3X_4X_5$) is the sum of the interaction weights for each (1,2) and (1,3) neighbor present. X_i is an amino acid; S_i is a structural digit that represents a region of (ϕ, ψ) space (described in (c) and (d)); $w_{S_iS_{i+1}}^{X_iX_{i+1}}$ is the weight for residues X_iX_{i+1} adopting structure S_iS_{i+1}; $w_{S_iS_{i+1}S_{i+2}}^{X_i\_X_{i+2}}$ is the weight for residues X_i and X_{i+2} adopting substructure $S_iS_{i+1}S_{i+2}$; and $w_Q^{X_1X_2X_3X_4X_5}$ is related to the partition function, Q, for sequence $X_1X_2X_3X_4X_5$ and ensures that all the structures' populations sum to 1 for a given sequence. (c) The (ϕ, ψ) population density of cyclo(L-Gly)$_5$. (d) The Ramachandran plot divided into 10 regions: *L*, *l*, *G*, *g*, *B*, *b*, *P*, *p*, *Z*, and *z*. For structural description based on the (ϕ, ψ) population density of cyclo(L-Gly)$_5$. Reproduced with permission from ref. 122 and 123 Copyright 2021, The Royal Society of Chemistry and 2023, American Chemical Society.

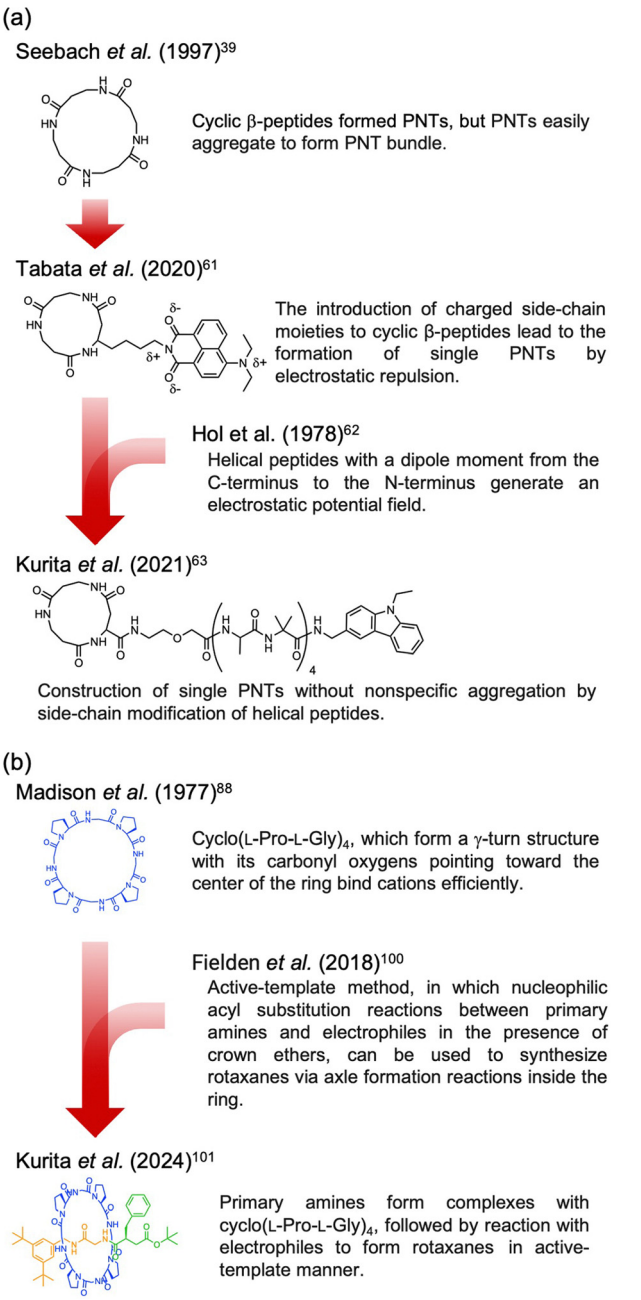

Fig. 18 Representative design protocols for rationally designed cyclic peptides, (a) cyclic β-peptides with helical peptides that form single PNTs and (b) cyclic peptides that form rotaxanes.

chains, is crucial for directing the assembly behaviors of PNTs and enabling precise control over their structural and functional properties. Such modifications both shape the hierarchical structure and increase the functionality of PNTs, thereby broadening their applications from organic electronics to innovative solutions for ion channels, antibacterial materials, and targeted delivery systems. The synthesis of rotaxanes using cyclic peptides represents a thrilling advancement, opening new frontiers in molecular architecture. Rationally designed cyclic peptides can interact with other molecules and forge pathways to develop mechanically interlocked molecular architectures. These dynamic structures have immense potential, revolutionizing everything from drug delivery systems to the development of molecular machines and materials with unprecedented mechanical properties.

The integration of computational tools and advanced simulation methods is expected to lead to significant breakthroughs in cyclic peptide research, enhancing both their understanding and application. These technologies not only increase our precision in predicting peptide behaviors but also innovate the way in which we design complex peptide structures. With cutting-edge sampling techniques, MD simulations will be crucial in unraveling the dynamic behaviors of cyclic peptides, fostering the development of new materials with enhanced properties. To fully

exploit the potential of cyclic peptides, cross-disciplinary collaboration that merges insights from synthetic chemistry, biology, and materials science into a cohesive research effort will be essential. Ultimately, the success of these endeavors rests on the sophisticated design of the primary structures of cyclic peptides, underscoring the pivotal role of molecular architecture in unlocking their full functional potential.

Author contributions

T. K. and K. N. contributed to the writing of this article.

Data availability

No primary research results, software or code have been included and no new data were generated or analysed as part of this review.

Conflicts of interest

The authors have no conflicts of interest to declare.

Acknowledgements

This research was financially supported by JST ERATO grant no. JPMJER1602, Japan (K. N.); Grant-in-Aid for Transformative Research Areas (B) grant no. JP20H05735 (K. N.); the MEXT Data Creation and Utilization-type MaTerial R&D project (K. N.); JST CREST grant no. JPMJCR2091 (K. N.) and JSPS Research Fellowships for Young Scientists (grant no. 23KJ1250 (K. T.)).

Notes and references

1 B. J. Pepe-Mooney and R. Fairman, *Curr. Opin. Struct. Biol.*, 2009, **19**, 483–494.
2 M. J. Harrington and P. Fratzl, *Prog. Mater. Sci.*, 2021, **120**, 1–40.
3 B. E. Ramakers, J. C. van Hest and D. W. Lowik, *Chem. Soc. Rev.*, 2014, **43**, 2743–2756.
4 R. V. Ulijn and A. M. Smith, *Chem. Soc. Rev.*, 2008, **37**, 664–675.
5 K. Numata, *Polym. J.*, 2015, **47**, 537–545.
6 G. Abbenante, D. R. March, D. A. Bergman, P. A. Hunt, B. Garnham, R. J. Dancer, J. L. Martin and D. P. Fairlie, *J. Am. Chem. Soc.*, 1995, **117**, 10220–10226.
7 H. L. Sham, C. A. Rempel, H. Stein and J. Cohen, *J. Chem. Soc., Chem. Commun.*, 1990, 666–667.
8 R. M. Schultz, J. P. Huff, P. Anagnostaras, U. Olsher and E. R. Blout, *Int. J. Pept. Protein Res.*, 1982, **19**, 454–469.
9 J. Witek, S. Wang, B. Schroeder, R. Lingwood, A. Dounas, H. J. Roth, M. Fouche, M. Blatter, O. Lemke, B. Keller and S. Riniker, *J. Chem. Inf. Model.*, 2019, **59**, 294–308.
10 S. Ono, M. R. Naylor, C. E. Townsend, C. Okumura, O. Okada and R. S. Lokey, *J. Chem. Inf. Model.*, 2019, **59**, 2952–2963.
11 J. Witek, M. Muhlbauer, B. G. Keller, M. Blatter, A. Meissner, T. Wagner and S. Riniker, *ChemPhysChem*, 2017, **18**, 3309–3314.
12 J. Witek, B. G. Keller, M. Blatter, A. Meissner, T. Wagner and S. Riniker, *J. Chem. Inf. Model.*, 2016, **56**, 1547–1562.
13 B. Over, P. Matsson, C. Tyrchan, P. Artursson, B. C. Doak, M. A. Foley, C. Hilgendorf, S. E. Johnston, M. D. T. Lee, R. J. Lewis, P. McCarren, G. Muncipinto, U. Norinder, M. W. Perry, J. R. Duvall and J. Kihlberg, *Nat. Chem. Biol.*, 2016, **12**, 1065–1074.
14 Q. Song, Z. Cheng, M. Kariuki, S. C. L. Hall, S. K. Hill, J. Y. Rho and S. Perrier, *Chem. Rev.*, 2021, **121**, 13936–13995.
15 R. J. Brea, C. Reiriz and J. R. Granja, *Chem. Soc. Rev.*, 2010, **39**, 1448–1456.
16 B. J. Pieters, M. B. van Eldijk, R. J. Nolte and J. Mecinovic, *Chem. Soc. Rev.*, 2016, **45**, 24–39.
17 J. M. Alonso, M. L. Gorzny and A. M. Bittner, *Trends Biotechnol.*, 2013, **31**, 530–538.
18 A. Harada, J. Li and M. Kamachi, *Nature*, 1993, **364**, 516–518.
19 T. Shimizu, M. Masuda and H. Minamikawa, *Chem. Rev.*, 2005, **105**, 1401–1443.
20 T. Shimizu, H. Minamikawa, M. Kogiso, M. Aoyagi, N. Kameta, W. Ding and M. Masuda, *Polym. J.*, 2014, **46**, 831–858.
21 C. H. Gorbitz, *Chem. – Eur. J.*, 2001, **7**, 5153–5159.
22 T. Kanzaki, Y. Horikawa, A. Makino, J. Sugiyama and S. Kimura, *Macromol. Biosci.*, 2008, **8**, 1026–1033.
23 W. H. Hsieh and J. Liaw, *J. Food Drug Anal.*, 2019, **27**, 32–47.
24 H. Y. Chow, Y. Zhang, E. Matheson and X. Li, *Chem. Rev.*, 2019, **119**, 9971–10001.
25 M. R. Ghadiri, J. R. Granja, R. A. Milligan, D. E. McRee and N. Khazanovich, *Nature*, 1993, **366**, 324–327.
26 D. Seebach, M. Overhand, F. N. M. Kühnle, B. Martinoni, L. Oberer, U. Hommel and H. Widmer, *Helv. Chim. Acta*, 1996, **79**, 913–941.
27 M. Amorin, L. Castedo and J. R. Granja, *J. Am. Chem. Soc.*, 2003, **125**, 2844–2845.
28 M. E. Polaskova, J. N. Lambert and N. J. Ede, *Aust. J. Chem.*, 1998, **51**, 535.
29 M. Saviano, L. Zaccaro, A. Lombardi, C. Pedone, B. Blasio, X. Sun and G. P. Lorenzi, *J. Inclusion Phenom. Mol. Recognit. Chem.*, 1994, **18**, 27–36.
30 X. Sun and G. P. Lorenzi, *Helv. Chim. Acta*, 1994, **77**, 1520–1526.
31 M. R. Ghadiri, K. Kobayashi, J. R. Granja, R. K. Chadha and D. E. McRee, *Angew. Chem., Int. Ed. Engl.*, 1995, **34**, 93–95.
32 T. D. Clark, J. M. Buriak, K. Kobayashi, M. P. Isler, D. E. McRee and M. R. Ghadiri, *J. Am. Chem. Soc.*, 1998, **120**, 8949–8962.
33 K. Kobayashi, J. R. Granja and M. R. Ghadiri, *Angew. Chem., Int. Ed. Engl.*, 1995, **34**, 95–98.
34 M. R. Silk, J. Newman, J. C. Ratcliffe, J. F. White, T. Caradoc-Davies, J. R. Price, S. Perrier, P. E. Thompson and D. K. Chalmers, *Chem. Commun.*, 2017, **53**, 6613–6616.

35 J. D. Hartgerink, J. R. Granja, R. A. Milligan and M. R. Ghadiri, *J. Am. Chem. Soc.*, 1996, **118**, 43–50.
36 I. Insua and J. Montenegro, *J. Am. Chem. Soc.*, 2020, **142**, 300–307.
37 I. Insua, A. Cardellini, S. Diaz, J. Bergueiro, R. Capelli, G. M. Pavan and J. Montenegro, *Chem. Sci.*, 2023, **14**, 14074–14081.
38 R. P. Cheng, S. H. Gellman and W. F. DeGrado, *Chem. Rev.*, 2001, **101**, 3219–3232.
39 D. Seebach, J. L. Matthews, A. Meden, T. Wessels, C. Baerlocher and L. B. McCusker, *Helv. Chim. Acta*, 2004, **80**, 173–182.
40 H. Uji, T. Morita and S. Kimura, *Phys. Chem. Chem. Phys.*, 2013, **15**, 757–760.
41 S. Yasutomi, T. Morita, Y. Imanishi and S. Kimura, *Science*, 2004, **304**, 1944–1947.
42 T. Morita, S. Kimura, S. Kobayashi and Y. Imanishi, *J. Am. Chem. Soc.*, 2000, **122**, 2850–2859.
43 T. D. Clark, L. K. Buehler and M. R. Ghadiri, *J. Am. Chem. Soc.*, 1998, **120**, 651–656.
44 W. S. Horne, N. Ashkenasy and M. R. Ghadiri, *Chem. – Eur. J.*, 2005, **11**, 1137–1144.
45 N. Ashkenasy, W. S. Horne and M. R. Ghadiri, *Small*, 2006, **2**, 99–102.
46 H. Uji, H. Kim, T. Imai, S. Mitani, J. Sugiyama and S. Kimura, *Biopolymers*, 2016, **106**, 275–282.
47 R. J. Brea, M. E. Vazquez, M. Mosquera, L. Castedo and J. R. Granja, *J. Am. Chem. Soc.*, 2007, **129**, 1653–1657.
48 C. Reiriz, R. J. Brea, R. Arranz, J. L. Carrascosa, A. Garibotti, B. Manning, J. M. Valpuesta, R. Eritja, L. Castedo and J. R. Granja, *J. Am. Chem. Soc.*, 2009, **131**, 11335–11337.
49 Y. Kamano, Y. Tabata, H. Uji and S. Kimura, *RSC Adv.*, 2019, **9**, 3618–3624.
50 Y. Tabata, S. Mitani and S. Kimura, *J. Pept. Sci.*, 2016, **22**, 391–396.
51 H. Ohmura, Y. Tabata, S. Kimura and H. Uji, *Pept. Sci.*, 2020, **113**, 1–8.
52 L. Atzori, A. Iera and G. Morabito, *Comput. Networks*, 2010, **54**, 2787–2805.
53 R. Bogue, *Sens. Rev.*, 2014, **34**, 137–142.
54 Y. Sun, K. Y. Zeng and T. Li, *Sci. China: Phys., Mech. Astron.*, 2020, **63**, 278701.
55 H. Yuan, P. Han, K. Tao, S. Liu, E. Gazit and R. Yang, *Research*, 2019, **2019**, 1–13.
56 B. Y. Lee, J. Zhang, C. Zueger, W. J. Chung, S. Y. Yoo, E. Wang, J. Meyer, R. Ramesh and S. W. Lee, *Nat. Nanotechnol.*, 2012, **7**, 351–356.
57 Y. Tabata, S. Mitani, H. Uji, T. Imai and S. Kimura, *Polym. J.*, 2019, **51**, 601–609.
58 Y. Tabata, Y. Kamano, H. Uji, T. Imai and S. Kimura, *Chem. Lett.*, 2019, **48**, 322–324.
59 Y. Ishihara and S. Kimura, *J. Pept. Sci.*, 2010, **16**, 110–114.
60 Y. Ishihara and S. Kimura, *Biopolymers*, 2013, **100**, 141–147.
61 Y. Tabata, Y. Kamano, S. Kimura and H. Uji, *RSC Adv.*, 2020, **10**, 3588–3592.
62 W. G. Hol, P. T. van Duijnen and H. J. Berendsen, *Nature*, 1978, **273**, 443–446.
63 T. Kurita, T. Terabayashi, S. Kimura, K. Numata and H. Uji, *Biomacromolecules*, 2021, **22**, 2815–2821.
64 F. Fujimura, T. Hirata, T. Morita, S. Kimura, Y. Horikawa and J. Sugiyama, *Biomacromolecules*, 2006, **7**, 2394–2400.
65 T. Hirata, F. Fujimura and S. Kimura, *Chem. Commun.*, 2007, 1023–1025.
66 F. Fujimura, Y. Horikawa, T. Morita, J. Sugiyama and S. Kimura, *Biomacromolecules*, 2007, **8**, 611–616.
67 R. J. Brea, M. Amorin, L. Castedo and J. R. Granja, *Angew. Chem., Int. Ed.*, 2005, **44**, 5710–5713.
68 R. J. Brea, L. Castedo, J. R. Granja, M. Á. Herranz, L. Sánchez, N. Martín, W. Seitz and D. M. Guldi, *Proc. Natl. Acad. Sci. U. S. A.*, 2007, **104**, 5291–5294.
69 M. Calvelo, A. Lamas, A. Guerra, M. Amorin, R. Garcia-Fandino and J. R. Granja, *Chem. – Eur. J.*, 2020, **26**, 5846–5858.
70 N. Rodríguez-Vázquez, M. Amorín, I. Alfonso and J. R. Granja, *Angew. Chem., Int. Ed.*, 2016, **55**, 4504–4508.
71 N. Rodriguez-Vazquez, R. Garcia-Fandino, M. Amorin and J. R. Granja, *Chem. Sci.*, 2016, **7**, 183–187.
72 H. L. Ozores, M. Amorin and J. R. Granja, *J. Am. Chem. Soc.*, 2017, **139**, 776–784.
73 B. H. Gan, J. Gaynord, S. M. Rowe, T. Deingruber and D. R. Spring, *Chem. Soc. Rev.*, 2021, **50**, 7820–7880.
74 N. Lawrence, G. J. Philippe, P. J. Harvey, N. D. Condon, A. H. Benfield, O. Cheneval, D. J. Craik and S. Troeira Henriques, *RSC. Chem. Biol.*, 2020, **1**, 405–420.
75 X. Luan, Y. Wu, Y. W. Shen, H. Zhang, Y. D. Zhou, H. Z. Chen, D. G. Nagle and W. D. Zhang, *Nat. Prod. Rep.*, 2021, **38**, 7–17.
76 H. Zhang and S. Chen, *RSC. Chem. Biol.*, 2022, **3**, 18–31.
77 V. T. Ivanov, A. I. Miroshnikov, N. D. Abdullaev, L. B. Senyavina, S. F. Arkhipova, N. N. Uvarova, K. K. Khalilulina, V. F. Bystrov and Y. A. Ovchinnikov, *Biochem. Biophys. Res. Commun.*, 1971, **42**, 654–663.
78 R. P. Daniele and S. K. Holian, *Proc. Natl. Acad. Sci. U. S. A.*, 1976, **73**, 3599–3602.
79 L. Becucci, M. R. Moncelli, R. Naumann and R. Guidelli, *J. Am. Chem. Soc.*, 2005, **127**, 13316–13323.
80 E. E. Ross, B. Hoag, I. Joslin and T. Johnston, *Langmuir*, 2019, **35**, 9410–9421.
81 J. R. Aviles-Moreno, F. Gamez, G. Berden, J. Martens, J. Oomens and B. Martinez-Haya, *Phys. Chem. Chem. Phys.*, 2020, **22**, 19725–19734.
82 K. D. Kopple, A. Go, T. J. Schamper and C. S. Wilcox, *J. Am. Chem. Soc.*, 1973, **95**, 6090–6096.
83 K. D. Kopple, T. J. Schamper and A. Go, *J. Am. Chem. Soc.*, 1974, **96**, 2597–2605.
84 L. M. Gierasch, C. M. Deber, V. Madison, C. H. Niu and E. R. Blout, *Biochemistry*, 1981, **20**, 4730–4738.
85 D. S. Eggleston, P. W. Baures, C. E. Peishoff and K. D. Kopple, *J. Am. Chem. Soc.*, 1991, **113**, 4410–4416.
86 V. Madison, M. Atreyi, C. M. Deber and E. R. Blout, *J. Am. Chem. Soc.*, 1974, **96**, 6725–6734.

87 M. Hollosi and T. Wieland, *Int. J. Pept. Protein Res.*, 1977, **10**, 329–341.
88 V. Madison, C. M. Deber and E. R. Blout, *J. Am. Chem. Soc.*, 1977, **99**, 4788–4798.
89 I. L. Karle, J. Karle, T. Wieland, W. Burgermeister, H. Faulstich and B. Witkop, *Proc. Natl. Acad. Sci. U. S. A.*, 1973, **70**, 1836–1840.
90 J. D. Gregory and L. C. Craig, *J. Biol. Chem.*, 1948, **172**, 839.
91 L. R. Gahan and R. M. Cusack, *Polyhedron*, 2018, **153**, 1–23.
92 Z. Liu, S. K. M. Nalluri and J. F. Stoddart, *Chem. Soc. Rev.*, 2017, **46**, 2459–2478.
93 M. J. Bayro, J. Mukhopadhyay, G. V. Swapna, J. Y. Huang, L. C. Ma, E. Sineva, P. E. Dawson, G. T. Montelione and R. H. Ebright, *J. Am. Chem. Soc.*, 2003, **125**, 12382–12383.
94 O. Pavlova, J. Mukhopadhyay, E. Sineva, R. H. Ebright and K. Severinov, *J. Biol. Chem.*, 2008, **283**, 25589–25595.
95 M. O. Maksimov, S. J. Pan and A. James Link, *Nat. Prod. Rep.*, 2012, **29**, 996–1006.
96 Y. Okumura and K. Ito, *Adv. Mater.*, 2001, **13**, 485–487.
97 J. Sawada, D. Aoki, S. Uchida, H. Otsuka and T. Takata, *ACS Macro Lett.*, 2015, **4**, 598–601.
98 V. Aucagne, D. A. Leigh, J. S. Lock and A. R. Thomson, *J. Am. Chem. Soc.*, 2006, **128**, 1784–1785.
99 A. Moretto, M. Crisma, F. Formaggio and C. Toniolo, *Biomol. Concepts*, 2012, **3**, 183–192.
100 S. D. P. Fielden, D. A. Leigh, C. T. McTernan, B. Perez-Saavedra and I. J. Vitorica-Yrezabal, *J. Am. Chem. Soc.*, 2018, **140**, 6049–6052.
101 T. Kurita, M. Higashi, J. Gimenez-Dejoz, S. Fujita, H. Uji, H. Sato and K. Numata, *Biomacromolecules*, 2024, **25**, 3661–3670.
102 R. T. Lam, A. Belenguer, S. L. Roberts, C. Naumann, T. Jarrosson, S. Otto and J. K. Sanders, *Science*, 2005, **308**, 667–669.
103 Y. Sugita and Y. Okamoto, *Chem. Phys. Lett.*, 1999, **314**, 141–151.
104 S. Piana and A. Laio, *J. Phys. Chem. B*, 2007, **111**, 4553–4559.
105 N. Nakajima, H. Nakamura and A. Kidera, *J. Phys. Chem. B*, 1997, **101**, 817–824.
106 D. Hamelberg, J. Mongan and J. A. McCammon, *J. Chem. Phys.*, 2004, **120**, 11919–11929.
107 A. Shkurti, I. D. Styliari, V. Balasubramanian, I. Bethune, C. Pedebos, S. Jha and C. A. Laughton, *J. Chem. Theory Comput.*, 2019, **15**, 2587–2596.
108 J. Damjanovic, J. Miao, H. Huang and Y. S. Lin, *Chem. Rev.*, 2021, **121**, 2292–2324.
109 D. P. Slough, S. M. McHugh, A. E. Cummings, P. Dai, B. L. Pentelute, J. A. Kritzer and Y. S. Lin, *J. Phys. Chem. B*, 2018, **122**, 3908–3919.
110 A. E. Cummings, J. Miao, D. P. Slough, S. M. McHugh, J. A. Kritzer and Y. S. Lin, *Biophys. J.*, 2019, **116**, 433–444.
111 F. Fonseca Lopez, J. Miao, J. Damjanovic, L. Bischof, M. B. Braun, Y. Ling, M. D. Hartmann, Y. S. Lin and J. A. Kritzer, *J. Chem. Inf. Model.*, 2023, **63**, 6925–6937.
112 S. M. McHugh, J. R. Rogers, H. T. Yu and Y. S. Lin, *J. Chem. Theory Comput.*, 2016, **12**, 2480–2488.
113 S. M. McHugh, H. Yu, D. P. Slough and Y. S. Lin, *Phys. Chem. Chem. Phys.*, 2017, **19**, 3315–3324.
114 M. C. Lu, Z. Y. Chen, Y. L. Wang, Y. L. Jiang, Z. W. Yuan, Q. D. You and Z. Y. Jiang, *RSC Adv.*, 2015, **5**, 85983–85987.
115 P. Bryant, G. Pozzati and A. Elofsson, *Nat. Commun.*, 2022, **13**, 1265.
116 P. Bryant, G. Pozzati, W. Zhu, A. Shenoy, P. Kundrotas and A. Elofsson, *Nat. Commun.*, 2022, **13**, 6028.
117 J. Abramson, J. Adler, J. Dunger, R. Evans, T. Green, A. Pritzel, O. Ronneberger, L. Willmore, A. J. Ballard, J. Bambrick, S. W. Bodenstein, D. A. Evans, C. C. Hung, M. O'Neill, D. Reiman, K. Tunyasuvunakool, Z. Wu, A. Zemgulyte, E. Arvaniti, C. Beattie, O. Bertolli, A. Bridgland, A. Cherepanov, M. Congreve, A. I. Cowen-Rivers, A. Cowie, M. Figurnov, F. B. Fuchs, H. Gladman, R. Jain, Y. A. Khan, C. M. R. Low, K. Perlin, A. Potapenko, P. Savy, S. Singh, A. Stecula, A. Thillaisundaram, C. Tong, S. Yakneen, E. D. Zhong, M. Zielinski, A. Zidek, V. Bapst, P. Kohli, M. Jaderberg, D. Hassabis and J. M. Jumper, *Nature*, 2024, **630**, 493–500.
118 J. Jumper, R. Evans, A. Pritzel, T. Green, M. Figurnov, O. Ronneberger, K. Tunyasuvunakool, R. Bates, A. Zidek, A. Potapenko, A. Bridgland, C. Meyer, S. A. A. Kohl, A. J. Ballard, A. Cowie, B. Romera-Paredes, S. Nikolov, R. Jain, J. Adler, T. Back, S. Petersen, D. Reiman, E. Clancy, M. Zielinski, M. Steinegger, M. Pacholska, T. Berghammer, S. Bodenstein, D. Silver, O. Vinyals, A. W. Senior, K. Kavukcuoglu, P. Kohli and D. Hassabis, *Nature*, 2021, **596**, 583–589.
119 M. Baek, F. DiMaio, I. Anishchenko, J. Dauparas, S. Ovchinnikov, G. R. Lee, J. Wang, Q. Cong, L. N. Kinch, R. D. Schaeffer, C. Millan, H. Park, C. Adams, C. R. Glassman, A. DeGiovanni, J. H. Pereira, A. V. Rodrigues, A. A. van Dijk, A. C. Ebrecht, D. J. Opperman, T. Sagmeister, C. Buhlheller, T. Pavkov-Keller, M. K. Rathinaswamy, U. Dalwadi, C. K. Yip, J. E. Burke, K. C. Garcia, N. V. Grishin, P. D. Adams, R. J. Read and D. Baker, *Science*, 2021, **373**, 871–876.
120 R. Krishna, J. Wang, W. Ahern, P. Sturmfels, P. Venkatesh, I. Kalvet, G. R. Lee, F. S. Morey-Burrows, I. Anishchenko, I. R. Humphreys, R. McHugh, D. Vafeados, X. Li, G. A. Sutherland, A. Hitchcock, C. N. Hunter, A. Kang, E. Brackenbrough, A. K. Bera, M. Baek, F. DiMaio and D. Baker, *Science*, 2024, **384**, eadl2528.
121 S. A. Rettie, K. V. Campbell, A. K. Bera, A. Kang, S. Kozlov, J. De La Cruz, V. Adebomi, G. Zhou, F. DiMaio, S. Ovchinnikov and G. Bhardwaj, *bioRxiv*, 2023, preprint, DOI: 10.1101/2023.02.25.529956.
122 J. Miao, M. L. Descoteaux and Y. S. Lin, *Chem. Sci.*, 2021, **12**, 14927–14936.
123 T. Hui, M. L. Descoteaux, J. Miao and Y. S. Lin, *J. Chem. Theory Comput.*, 2023, **19**, 4757–4769.